Hedging of Asian options under exponential Lévy models: computation and performance

Laura Ballotta[*][1], Russell Gerrard[2], and Ioannis Kyriakou[2]

[1]Faculty of Finance

[2]Faculty of Actuarial Science and Insurance

Cass Business School, City University London, UK

June 2015

Abstract

In this paper we consider the problem of hedging an arithmetic Asian option with discrete monitoring in an exponential Lévy model by deriving backward recursive integrals for the price sensitivities of the option. The procedure is applied to the analysis of the performance of the delta and delta-gamma hedges in an incomplete market; particular attention is paid to the hedging error and the impact of model error on the quality of the chosen hedging strategy. The numerical analysis shows the impact of jump risk on the hedging error of the option position, and the importance of including traded options in the hedging portfolio for the reduction of this risk.

Keywords: Arithmetic Asian options, Discrete monitoring, Price sensitivities, Lévy processes, Hedging error, Model misspecification

JEL Classification: G13, G11, D52, C63

[*]Corresponding Author: Email: L.Ballotta@city.ac.uk

1   Introduction

In this paper we investigate the problem of computing the price sensitivities of European arithmetic Asian options with discrete monitoring, and the performance of the resulting hedging portfolios in terms of reduction of the option's risk exposure. To this purpose, we derive a method for computing the option price sensitivities (like delta and gamma) and study the impact of ignoring the probability of shocks occurring to the underlying asset price during the contract's lifetime.

Practitioners are interested in accurate and efficient ways to calculate the prices of derivative contracts, but also their sensitivities (also known as the 'Greeks') obtained by differentiating the contract price with respect to parameters of interest. Common Greeks are the so-called delta and gamma, which represent the first and second derivatives of the contract price with respect to the value of the underlying, S_0, and the vega which is given by the first derivative of the contract price with respect to the volatility of the underlying. The Greeks are used to construct portfolios aimed at hedging the exposure originated by the corresponding option contract by trading in the underlying asset and/or other options. Their appeal stems from the fact that they lead to linear hedging rules, a desirable feature in that it allows reducing significantly the computational cost of hedging a book of options written on the same underlying.

Asian options are derivative contracts written on the arithmetic average value of the underlying which trade frequently in various markets, including the equity (e.g., see Fusai and Meucci, 2008), commodity (e.g., see Fusai et al., 2008), currency (e.g., see Lo et al., 2008) and freight (e.g., see Nomikos et al., 2013) markets. Their appeal stems mainly from the fact that, as the payoff depends on the average value of the underlying, the risk of market manipulations as the contract approaches maturity is reduced. As the recent events in the financial markets have highlighted the importance of capturing market shocks using more refined distribution assumptions compared to the standard Black–Scholes framework, in this paper we consider the case of an underlying asset modelled according to an exponential Lévy process, and analyze the potential error caused by incorrectly specifying the underlying asset distribution

features on the hedging of a book of Asian options.

Exponential Lévy models generally correspond to incomplete markets due to the introduction of discontinuities in the asset prices trajectories. Hedging under these conditions presents a number of challenges. In first place, hedging can no longer be interpreted as exact replication, like in the Black–Scholes model, but only as an approximation of the terminal payoff offered by the contract under consideration. In this context, in fact, the classical delta hedge is known to be sub-optimal as it does not eliminate risk completely; this implies the introduction of a non-trivial hedging error in form of residual risk from the original exposure. A popular alternative approach is the so-called quadratic hedging which, broadly speaking, aims at minimizing the expected squared deviation of the hedging portfolio from the contingent claim (for fuller details on quadratic hedging, we refer for example to Tankov, 2010; Goutte et al., 2013, 2014, and references therein). However, Greeks-based hedging strategies like, for example, delta and delta-gamma hedges are still commonly used in practice; in particular, the delta hedge is shown to generate an error which is relatively close to the one produced by quadratic hedging (see Denkl et al., 2013; Cont et al., 2007, amongst others). For the case of a discretely sampled Asian option, an additional challenge is due to the lack of analytical solution for the contract price, and hence its sensitivities.

Over the last few years fast and accurate algorithms emerged for pricing European discrete arithmetic Asian options beyond the traditional lognormal asset price model; we mention, amongst others, Černý and Kyriakou (2011), Fusai and Meucci (2008), Fusai et al. (2008), Fusai et al. (2011), Marena et al. (2013) and Zhang and Oosterlee (2013). Whereas the pricing of Asian options is well-understood, an additional interesting direction to explore is that of the computation of the price sensitivities, which poses the main challenge of proving validity of the interchange of differentiation and the integral price representation.

In light of the previous discussion, the contribution of our paper is two-fold. Firstly, we develop a method for computing the price sensitivities of the European Asian option using backward recursive convolutions. In more details, our approach is based on direct differentiation of the risk neutral conditional expectation of the discounted payoff of the Asian option expressed in terms of the so-called Carverhill–Clewlow–Hodges factorization. Assuming a

generic process with independent increments for the log-returns of the underlying, we prove that differentiation under the integral sign with respect to parameters of interest is permissible. In particular, we reach general solutions for the option's delta and gamma (Theorem 1), but also the non-trivial case of the option's vega for a lognormal underlying (Theorem 2); en route, we prove that the vega of the given contract is positive, extending the results of Carr et al. (2008) from the case of a continuously to a discretely monitored arithmetic Asian option. It is worth pointing out that the suggested method can give access to any other price sensitivity, providing that differentiation under the integral sign is allowed. The accuracy of our method is demonstrated by numerical tests performed under different Lévy models for the asset log-returns, like the Brownian motion, the Normal Inverse Gaussian (NIG) model (Barndorff-Nielsen, 1995) and the Carr–Geman–Madan–Yor (CGMY) model (Carr et al., 2002); we also provide a comparison against the outcome from Monte Carlo simulations. Secondly, we use the proposed method to set up the delta and delta-gamma hedging portfolios for the Asian option under consideration, and investigate their performance in the incomplete market originated by the adopted exponential Lévy models. In particular, we pay attention to the goodness of the approximation of the terminal payoff of the contract and the behaviour of the residual risk, i.e. the hedging error. We also study the impact of misspecifying the underlying asset price dynamics on the performance of the Greeks-based hedging portfolios, which we refer to as model error.

The outline of the paper is as follows. In Section 2 we present our main theoretical findings on the computation of the price sensitivities of Asian options. In Section 3 we present the results from the numerical implementation of the proposed method; the procedure is benchmarked against Monte Carlo (with control variate). In Section 4 we illustrate the performance of Greeks-based hedges (like the delta and delta-gamma portfolios) in terms of hedging error and model error. Section 5 concludes. All the proofs are deferred to the appendices.

2 Recursive integrals for Asian option sensitivities

2.1 Backward price recursion

Consider an Asian option with underlying S observed over the period $(0, T]$ at the equidistant times $t_1 = \delta, t_2 = 2\delta, \ldots, t_n = n\delta = T$. Let $\{Z_k\}_{k=1}^n$ be a collection of independent random variables representing the log-returns on S, such that

$$S_j = S_0 \exp\left(\sum_{k=1}^j Z_k\right), \ j = 1, \ldots, n, \ S_0 > 0.$$

The sequence $\{Z_k\}_{k=1}^n$ can be thought of, for example, as the increments of a specific Lévy process, such as the Brownian motion, the NIG process or the CGMY process.

Under the unified framework of Večeř (2002), the payoff of an Asian option is generally given by

$$\left(\sum_{k=0}^n \lambda_k S_k\right)^+, \tag{1}$$

where $(\cdot)^+$ is the positive part function and coefficients $\{\lambda_k\}_{k=0}^n$ are deterministic and take different values for different contract specifications. For example, for

$$\lambda_0 := -\frac{K}{S_0} \text{ and } \lambda_k := \frac{1}{n}, \ 0 < k \leq n, \tag{2}$$

we retrieve the payoff of the call option with fixed strike price $K > 0$

$$\left(\sum_{k=1}^n \lambda_k S_k\right)^+ = \left(\frac{1}{n} \sum_{k=1}^n S_k - K\right)^+.$$

Define the reverse filtration $\mathbb{G} = \{\mathcal{G}_k\}_{k=1}^n$ for $\mathcal{G}_k = \sigma\{Z_n, Z_{n-1}, \ldots, Z_{n+1-k}\}$, and consider the process

$$Y_k = \ln(e^{Y_{k-1}} + \lambda_{n+1-k}) + Z_{n+1-k}, \ 1 < k \leq n, \tag{3}$$

$$Y_1 = \ln \lambda_n + Z_n, \tag{4}$$

with $\lambda_k > 0$, $0 < k \leq n$. On evaluating $\exp(Y_k)$ recursively using (3)–(4), we can factorize (1) as $S_0(e^{Y_n} + \lambda_0)^+$, where $\lambda_0 \in \mathbb{R}$. (This factorization result has been contributed by Stewart Hodges and first appeared in Carverhill and Clewlow, 1990.)

Without loss of generality, we focus here on the call option with fixed strike price satisfying (2). Then, given the price of the fixed strike call, the price of the floating strike put option can be obtained using a symmetry relationship derived in Eberlein and Papapantoleon (2005) for underlyings driven by exponential Lévy models, while the prices of the fixed strike put and floating strike call options can be obtained via standard put-call parity (e.g., see Fusai et al., 2011).

As the process Y is Markov in the filtration $\mathbb{G}$, the forward price of the option $E((S_0 e^{Y_n} - K)^+)$ under some risk neutral measure P can be computed recursively on a one-dimensional grid. To this end, assume that for all k the random variables Z_{n+1-k} have density functions f_k. For any $S_0 > 0$ and fixed $K > 0$, define

$$p_n(y) = S_0(e^y + \lambda_0)^+ = (S_0 e^y - K)^+. \tag{5}$$

Further, define recursively

$$\tilde{p}_{k-1}(x) = \int_{-\infty}^{\infty} p_k(x + z) f_k(z) dz, \ 0 < k \leq n, \tag{6}$$

$$p_k(y) = \tilde{p}_k(h_k(y)), \ 0 < k < n, \tag{7}$$

where

$$h_k(y) = \ln(e^y + \lambda_{n-k}), \ 0 < k < n. \tag{8}$$

It is shown in Černý and Kyriakou (2011, Theorem 3.1) that

$$0 \ \leq \ p_k(y) \leq a_k + b_k e^y, \tag{9}$$

$$0 \ \leq \ \tilde{p}_k(x) \leq a_{k+1} + b_k e^x, \tag{10}$$

where

$$a_n = 0, \ b_n = S_0, \tag{11}$$

$$a_k = a_{k+1} + b_k \lambda_{n-k}, \ b_k = b_{k+1} \mu_{k+1} \tag{12}$$

for

$$\mu_k := E(e^{Z_{n+1-k}}) = \int_{-\infty}^{\infty} e^z f_k(z) dz < \infty.$$

The forward price of an Asian call option with coefficients $\{\lambda_k\}$ as in (2) is given by

$$E((S_0 e^{Y_n} - K)^+) = \tilde{p}_0(\ln \lambda_n). \tag{13}$$

2.2 Delta and gamma recursions

In this section we show that, by direct differentiation of the risk neutral valuation formula (13) with respect to the initial asset value S_0, we are able to derive backward recursive convolutions that produce the exact Asian call option's delta and gamma sensitivities. For this to be feasible, we need first to guarantee differentiation under the integral sign. These results are proved in the following.

Theorem 1 *Assume S_0 lies on a bounded interval of the positive real axis. Suppose that, in addition to $\mu_k < \infty$, $\bar{\mu}_k := E(e^{-Z_{n+1-k}}) = \int_{-\infty}^{\infty} e^{-z} f_k(z) dz < \infty$ for all k. Consider the sequence of functions (5)–(8). The following statements hold.*

(i) There exists a sequence of non-negative constants given by

$$\alpha_n = 0, \ \beta_n = 1,$$

$$\alpha_k = \alpha_{k+1} + \beta_k \lambda_{n-k}, \ \beta_k = \beta_{k+1} \mu_{k+1},$$

such that

$$0 \leq \frac{\partial}{\partial S_0} p_k(y; S_0) \leq \alpha_k + \beta_k e^y \ \text{for } k \leq n, \tag{14}$$

$$0 \leq \frac{\partial}{\partial S_0} \tilde{p}_k(x; S_0) \leq \alpha_{k+1} + \beta_k e^x \ \text{for } k < n,$$

for all y and x.

(ii) For $k \leq n-1$,

$$\frac{\partial^2}{\partial S_0^2} p_k(y; S_0), \frac{\partial^2}{\partial S_0^2} \tilde{p}_k(x; S_0) \geq 0$$

for all y and x.

Further, there exists a sequence of non-negative constants given by

$$\gamma_{n-1} = -\frac{\lambda_0}{S_0}, \ \varepsilon_{n-1} = -\frac{\lambda_0 \lambda_1}{S_0}, \ \zeta_{n-1} = 0, \ \eta_{n-1} = 0,$$

$$\gamma_k = \gamma_{k+1} + \zeta_{k+1} \mu_{k+1} \lambda_{n-k},$$

$$\varepsilon_k = \varepsilon_{k+1} \bar{\mu}_{k+1} + (\gamma_{k+1} + \eta_{k+1}) \lambda_{n-k} + \zeta_{k+1} \mu_{k+1} \lambda_{n-k}^2,$$

$$\zeta_k = \zeta_{k+1} \mu_{k+1},$$

$$\eta_k = \eta_{k+1} + \zeta_{k+1} \mu_{k+1} \lambda_{n-k},$$

such that over any compact interval $y \in [L, U] \subset \mathbb{R}$

$$\int_L^U \frac{\partial^2}{\partial S_0^2} p_k(y; S_0) dy \leq \gamma_k + \varepsilon_k e^{-L} + \zeta_k e^U + \eta_k e^{U-L} \ \text{for } k \leq n-1. \tag{15}$$

(iii) There exists a sequence of functions given by

$$\frac{\partial}{\partial S_0} p_n(y; S_0) = e^y 1_{y > \ln(-\lambda_0)},$$

$$\frac{\partial^2}{\partial S_0^2} p_{n-1}(y; S_0) = -\frac{\lambda_0}{S_0} f_n \left(\ln \left(-\frac{\lambda_0}{e^y + \lambda_1} \right) \right)$$

and

$$\frac{\partial^j}{\partial S_0^j} \tilde{p}_{k-1}(x; S_0) = \int_{-\infty}^{\infty} \frac{\partial^j}{\partial S_0^j} p_k(x + z; S_0) f_k(z) dz, \tag{16}$$

$$\frac{\partial^j}{\partial S_0^j} p_k(y; S_0) = \frac{\partial^j}{\partial S_0^j} \tilde{p}_k(h_k(y); S_0)$$

for all x and y, and $j = 1$ and 2. The forward delta and gamma of the Asian call

option are given by

$$\frac{\partial^j}{\partial S_0^j} \tilde{p}_0(\ln \lambda_n; S_0)$$

for $j = 1$ and 2, respectively.

Proof. See Appendix A. ∎

2.3 Vega recursion

In this section the Black–Scholes model is assumed, i.e. the log-returns $\{Z_{n+1-k}\}$ represent the increments of a Brownian motion with drift, and therefore are identically distributed and follow a normal distribution with mean $E(Z) = (r - \sigma^2/2)\delta$ and variance $\text{Var}(Z) = \sigma^2\delta$, where r and σ denote the continuously compounded risk free rate of interest and the volatility of the underlying, respectively. We derive the recursive convolution for the Asian call option's vega, i.e. the Greek with respect to the model-specific parameter σ. Similarly to the case presented in Section 2.2, we need to guarantee that direct differentiation of (13) is feasible. We note that, whereas the convolutions of Section 2.2 rely on the dependence of the terminal payoff function (5) on S_0, additional complexity emerges in the case of the vega due to the dependence of the log-returns probability density f on σ at every iteration.

Our result is tailored to normal distributed log-returns. However, providing that the interchange between integration and differentiation in (6) is permitted, similar recursions can be obtained for sensitivities with respect to parameters of other Lévy models for the log-returns, including, for example, the volatility parameters ν and γ of the NIG model (see Bayazit and Nolder, 2013; Corcuera et al., 2008) with characteristic exponent (19), or market parameters, like the risk free rate r (so-called rho sensitivity). Mixed sensitivities, for example, with respect to the initial asset value and volatility (so-called vanna sensitivity) can also be obtained. Additional results can be made available by the authors upon request.

Theorem 2 *Let σ be the volatility of the price of underlying in the Black–Scholes model. Assume that σ lies on a bounded interval of the positive real axis. Consider the sequence of functions (5)–(8) and bounds (9)–(10). The following statements hold.*

(i) *There exists a sequence of non-negative constants given by*

$$
\tilde{c}_{n-1} = 0, \ d_{n-1} = \frac{1}{\sqrt{2\pi}} S_0 \sqrt{\delta} e^{r\delta}, \ c_{n-1} = d_{n-1}\lambda_1,
$$

$$
\tilde{c}_k = c_{k+1} + a_{k+1}\left(\frac{1}{\sigma} + \frac{1}{4}\sigma\delta\right),
$$

$$
d_k = d_{k+1} + b_{k+1}\left(\frac{1}{\sigma} + \frac{1}{4}\sigma\delta\right),
$$

$$
c_k = \tilde{c}_k + d_k\lambda_{n-k},
$$

where the constants a_k, b_k are given by (11)–(12), such that

$$
0 \leq \frac{\partial}{\partial\sigma}\tilde{p}_k(x;\sigma) \leq \tilde{c}_k + d_k e^x
$$
$$
0 \leq \frac{\partial}{\partial\sigma}p_k(y;\sigma) \leq c_k + d_k e^y \tag{17}
$$

for $0 < k \leq n-1$, for all x and y.

(ii) *There exists a sequence of functions given by*

$$
\frac{\partial}{\partial\sigma}p_{n-1}(y;\sigma) = S_0\sqrt{\delta}e^{r\delta}(e^y + \lambda_1)\phi\left(\frac{\ln(-\frac{e^y+\lambda_1}{\lambda_0}) + (r + \frac{1}{2}\sigma^2)\delta}{\sigma\sqrt{\delta}}\right),
$$

where ϕ is the standard normal density function, and

$$
\frac{\partial}{\partial\sigma}\tilde{p}_{k-1}(x;\sigma) = \int_{-\infty}^{\infty}\left(\frac{\partial}{\partial\sigma}p_k(x+z;\sigma)f(z;\sigma) + p_k(x+z;\sigma)\frac{\partial}{\partial\sigma}f(z;\sigma)\right)dz, \tag{18}
$$
$$
\frac{\partial}{\partial\sigma}p_k(y;\sigma) = \frac{\partial}{\partial\sigma}\tilde{p}_k(h_k(y);\sigma),
$$

where $f(z;\sigma) := \phi\left((z - (r - \frac{1}{2}\sigma^2)\delta)/(\sigma\sqrt{\delta})\right)/(\sigma\sqrt{\delta})$. The forward vega of the Asian call option is given by

$$
\frac{\partial}{\partial\sigma}\tilde{p}_0(\ln\lambda_n;\sigma).
$$

Proof. See Appendix B. ∎

We note that the vega of the given contract is always positive (see Equation 17), which extends the findings of Carr et al. (2008) to the case of a discretely monitored arithmetic

Asian option.

3   Algorithm performance analysis

3.1   Implementation

For illustration purposes, we test the backward integral recursions for the delta and gamma in the case in which the log-returns of the underlying asset are governed by a Lévy process; specifically we consider the case of a Brownian motion with drift (standard Black–Scholes (BS) model), the NIG process and the CGMY process. The corresponding characteristic functions are

$$
\begin{aligned}
E(e^{iuZ_k}) &= e^{\psi(u)\delta}, \ \forall k, \\
\psi(u) &= iu(r - \hat{\psi}(-i)) + \hat{\psi}(u),
\end{aligned}
$$

where

$$
\begin{aligned}
\hat{\psi}_{\mathrm{BS}}(u) &= -\frac{1}{2}\sigma^2 u^2, \ \ \sigma > 0, \\
\hat{\psi}_{\mathrm{NIG}}(u) &= \frac{1}{\nu}(1 - \sqrt{1 - 2i\theta\nu u + \nu\gamma^2 u^2}), \ \ \theta \in \mathbb{R}, \nu, \gamma > 0, \\
\hat{\psi}_{\mathrm{CGMY}}(u) &= C\Gamma(-Y)((M - iu)^Y - M^Y + (G + iu)^Y - G^Y), \ \ C, M, G > 0, Y < 2.
\end{aligned}
\tag{19}
$$

We also analyze the case of the vega sensitivity in the Black–Scholes model.

We compute numerically the Greeks convolutions (16) and (18) by Fourier transform; this allows us to translate the density-based solutions to characteristic function-based ones which are faster to compute and rely on simpler expressions of characteristic functions as opposed to likely complicated (if available in closed form) density functions. More specifically, we refer to Theorem 3.2 and Section 4 of Černý and Kyriakou (2011), respectively, about the construction of the Fourier transforms and their discretization for a fast numerical implementation using the so-called chirp z-transform (see also Bluestein, 1968; Rabiner et al., 1969 and Černý, 2004), which is readily available in common numerical computing plat-

forms like Matlab. This powerful approach allows us to gauge explicitly the precision of the scheme and, by further exploiting its smooth convergence in the number of discretization points of the Fourier transforms, achieve highly accurate results as we show in the following section. Alternatively, one may consider using the maturity randomization algorithm presented in Fusai et al. (2011) or the parallel wavelet-based procedure of Corsaro et al. (2015) for potential speed-up gains with increasing monitoring frequency. Richardson extrapolation techniques also provide substantial CPU power saving when dealing with a large number of monitoring dates.

As a benchmark, we use the results from Monte Carlo simulations. In particular, we employ classical pathwise (PW) estimation for the delta and vega (see Curran, 1994, 1998; Broadie and Glasserman, 1996, for example). In the case of gamma, we use mixed likelihood ratio-pathwise (LRPW) estimation (i.e. utilize each of the LR and PW approaches for one order of differentiation) which induces lowest standard error (see Glasserman, 2004). The latter case requires access to the density function of the log-returns, which in the case of the NIG and CGMY distributions we retrieve by transform inversion as in Glasserman and Liu (2010). In addition, given the characteristic function of the log-geometric average which has been derived in Fusai and Meucci (2008) for general independent and identically distributed (i.i.d.) log-returns, one can compute geometric option sensitivities at high accuracy using, for example, the inverse-transform formula of Carr and Madan (1999). This allows us to use the geometric option sensitivities as control variates in the estimation of the arithmetic option sensitivities. Finally, we simulate the NIG process using its subordinated Brownian motion representation (e.g., see Glasserman, 2004), while for the CGMY dynamics we adopt the joint Monte Carlo-Fourier transform sampling scheme in Ballotta and Kyriakou (2014) based on direct simulation of the process increments.

Results are shown in the following section.

3.2 Results

We opt for Asian call options with fixed strikes $K = \{90, 100, 110\}$, time to maturity $T = 1$, and $n = 50$ monitoring (reset) dates. We assume an initial spot price $S_0 = 100$ and a risk

free rate $r = 0.04$. For illustration purposes, we use the calibration (to stock index option prices) results of Černý and Kyriakou (2011) to achieve target volatility Vol = $\{0.1, 0.3, 0.5\}$ for all models, in addition to a skewness coefficient of -0.5 and excess kurtosis of 0.7 for the NIG and CGMY models, see Panel (a) of Table 1.

In Panel (b) of Table 1, we list the numerical results for the Greeks of arithmetic Asian call options from the backward recursions implemented using the transform technique referred to in Section 3.1 and the control variate Monte Carlo (CVMC) simulations (we employ standard CVMC setup with the CV coefficient estimated using a pilot run, as detailed, for example, in Glasserman, 2004). Across strikes, models and volatility levels, we observe smooth monotone convergence in the number of discretization points of the integral recursions, similarly to Černý and Kyriakou (2011). We present results with accuracy to 6 decimals achieved in up to 1.5 seconds[1], which is sufficient for the purposes of our hedging strategy exercise in Section 4. By sake of exemplification, in Figure 2 we present on a log-log scale the convergence patterns of the computed deltas and gammas in the NIG, CGMY and Black–Scholes models and vegas in the Black–Scholes model for an at-the-money option (i.e., $S_0 = K = 100$) and the case of volatility Vol = 0.1 (see Panel (a) of Table 1). We observe that smoothly diminishing error patterns are preserved under both leptokurtic or normal log-returns which ensure convergence to the desired number of decimal places reported on the left side of Panel (b) of Table 1. These can be exploited to achieve even higher accuracies, e.g., up to 10 decimals, with minimal extra computational cost (up to 4 seconds) using Richardson extrapolation (e.g., see Andricopoulos et al., 2003). (More numerical results are available upon request by the authors.) We note that all computed Greeks using backward recursions fall into the 99% confidence intervals estimated using 100,000 Monte Carlo simulations. To further demonstrate the power of our approach, we compute (proofs are omitted) backward recursions for the sensitivities with respect to the volatility parameters ν and γ of the NIG model log-returns (see discussion in Section 2.3) as well as the mixed sensitivity with respect to S_0 and the volatility parameters ν and γ (vanna sensitivity). Figure 3 presents on a log-log scale smoothly diminishing error patterns of the computed sensitivities for an at-the-money

---

[1]Computational time corresponds to a Matlab 2010 implementation on a PC with Intel Core i3-3220 CPU @ 3.3GHz and 4GB of RAM.

option (i.e., $S_0 = K = 100$) and the case of Vol = 0.1 (see Panel (a) of Table 1). In this example, with 6-decimal-place accuracy, the vega wrt ν is 1.673078; wrt γ is 17.567563, whereas the vanna wrt ν is 0.142703; wrt γ is -1.263555.

In the case of vega, the performance of Monte Carlo simulation deteriorates generating vega estimates with high standard errors, whereas the backward convolution method remains consistently accurate and efficient. Given our highly precise results for the vega of the Asian option, it is then easy to verify that, across strikes and volatilities, these are consistently lower than the ones of the corresponding plain vanilla option which can be seen as a special case of the Asian option with a single monitoring date. Figure 1 shows the case of at-the-money options with different maturities and for different volatility levels. This confirms the lower sensitivity of the contract to the volatility of the underlying asset induced by averaging, which explains the interest of investors for this type of option.

4   Hedging strategies performance analysis

In the following we consider the problem of hedging the given arithmetic Asian call option contract using the option's Greeks computed with the scheme proposed in Section 2.

We begin by noting from the results reported in Panel (b) of Table 1 the difference between the values of delta and gamma obtained under the Black–Scholes model and the ones generated by the NIG and the CGMY processes, which can reach up to 24% in the case of delta and 20% in the case of gamma. On the other hand, the estimates of these two sensitivities are very close under the NIG and the CGMY, which is consistent with intuition given that the first four cumulants of the log-returns distribution are matched under the chosen parameters values. In this respect, we conclude that model error is less severe when shocks are incorporated, even if this might be done sub-optimally, i.e. by choosing for example an infinite variation process such as the NIG instead of a finite variation one such as the CGMY considered in this example (note the choice of $Y = 0.8 \in (0,1)$). Hence, for ease of exposition, in the remaining of this section we focus on the case of the NIG model for the analysis of the performance of Greeks-based hedging strategies in presence of jumps (similar results are obtained for the CGMY model and are available upon request).

The numerical experiment is in spirit similar to the one carried out in Yang et al. (2011) and is organized as follows. We generate 1,000 batches of 10,000 NIG trajectories monitored at the reset dates of the Asian option; for each batch we select those trajectories generating the 5% ('worst' case scenario), the 50% (the median) and the 95% ('best' case scenario) quantile of the arithmetic average price of the underlying entering the terminal option payoff. Along the selected quantile trajectories, we compute the option's delta and gamma over the contract term using the backward integral recursion presented in Section 2.2; results are presented in Section 4.1. Finally, the previously computed Greeks are used to construct the delta hedging portfolio and the delta-gamma hedging portfolio of the Asian option for the strikes and the volatility values considered in Section 3.2. As the market is incomplete and exact replication is not possible, hedging can only be interpreted as an approximation of the terminal payoff, and as such it leads to the introduction of non-trivial error. We analyze this hedging error in Section 4.2.

In order to study model error as well, i.e. the error originated by the fact that the hedge may be derived in a model differing from the one where it is eventually applied, we use the backward integral recursion developed in Section 2.2 to compute the delta, the gamma and the corresponding hedging portfolios of the Asian option also under the Black–Scholes economy, and compare their performance over the lifetime of the contract to the ones obtained under the NIG model. The analysis is presented in Section 4.3.

Finally, we note that the rebalancing of the hedging portfolio is performed at the monitoring dates of the Asian call option; this choice is motivated mainly by the attempt to conciliate the trade-off between accuracy of the hedging position (which from the theoretical point of view requires continuous rebalancing) and the transaction costs which the trader would incur by frequently re-adjusting the portfolio. For a detailed analysis of the error originated by discrete rebalancing as the one adopted in our analysis, we refer for example to Brodén and Tankov (2011) and Gobet and Makhlouf (2012).

In the remaining of this section we use the same parameters as in Section 3.2, which are reported in Panel (a) of Table 1.

4.1 Delta and gamma

The Asian call option delta is shown in Figure 4; it represents the rate of change of the option premium when the underlying asset price changes, and the number of shares required to maintain the overall traders' position delta neutral. The corresponding Asian call option gamma is shown in Figure 5; it represents the rate of change of the delta with respect to the underlying price, and therefore 'quantifies' the curvature of the option premium with respect to the price of the underlying. Gamma neutral positions in a convex hedging instrument (generally another option contract) are proportional to the gamma of the Asian contract.

Consistent with intuition, Figure 4 shows that, regardless of the quantile trajectory considered, the delta of the Asian call option depends on the moneyness of the contract: the more in-the-money the option, the higher the value of the delta. This reflects the probability of a non-zero payout at maturity from the option, and therefore determines the amount of underlying asset the traders require to hedge their position. Figure 4 also shows that, in general, the behaviour of the delta of in-the-money options does not change significantly across the different quantile scenarios; the deltas of at-the-money and out-of-the-money contracts are instead more sensitive to the underlying asset trajectory, as confirmed by the corresponding values of their gamma. Figure 5 in fact shows that, especially in correspondence of low volatility values, the gamma reaches its maximal value for at-the-money and out-of-the-money options; on the other hand, in-the-money contracts are relatively insensitive to second-order effects of changes in the underlying value.

In light of these results, we expect delta hedging portfolios to provide the required cover for in-the-money options, and to require instead frequent rebalancing aimed at reducing the residual risk in the case of at/out-of-the-money contracts. Hence, we also expect delta-gamma hedging portfolios to be more effective for these options.

Further, the delta, in general, decreases over the lifetime of the contract, i.e. at each reset date the traders unwind part of their delta position due to the combined effect of the weight of the setting (see de Weert, 2008, for example) and the reduction of the uncertainty about the terminal payoff. These results are consistent with the findings obtained for the standard Black–Scholes economy by Yang et al. (2011), who also report that the liquidation of the

position in the risky asset is seemingly linear especially for in-the-money options. We observe a similar feature in our case as well but only for low volatility levels of the underlying (see Panels 4a, 4d and 4g). Similarly, the gamma decreases to zero as we approach the maturity of the contract: the position in the hedging option is gradually liquidated, although the decay rate changes significantly across strikes, quantile trajectories and volatility levels to take full account of the convexity effect. In this respect, Figures 4 and 5 provide some information about the charm and the color of the Asian call option (i.e. the delta and gamma decay, e.g., see Garman, 1992).

Both delta and gamma are sensitive to the value of the underlying volatility used to calculate them (these sensitivities are formalized by the so-called vanna and zomma, e.g., see Webb, 1999). In particular, ceteris paribus, increasing the volatility increases the delta of out-of-the-money options, as the probability that the contracts might move in the money increases as well. We also note that the delta of in-the-money options loses the seemingly linear decay over time. Higher volatility levels produce generally lower gamma values (note the scale in the panels of Figure 5): the position in the hedging option is more conservative in more volatile market conditions.

4.2   Hedging error

We define the hedging error as the difference between the hedging portfolio at maturity and the arithmetic Asian call option's terminal payoff, expressed as a percentage of the (forward) option price. We compute this error in correspondence of all strikes, volatility values and quantile trajectories considered so far; results are shown in Figure 6.

In details, the top three panels of Figure 6 illustrate the hedging errors originated by the model delta portfolio, composed of delta units of the underlying asset and the investment in the risk free bond, for the given three volatility levels. Each panel shows the errors for the given moneyness levels and quantiles. The bottom three panels correspond instead to the hedging error originated by the model delta-gamma portfolio, obtained by combining the underlying asset and one European vanilla call option (in addition to the position in the risk free bond) in amounts fixed as to neutralize both the delta and the gamma of the overall

position. The vanilla option used for the gamma hedge has the same underlying asset as the arithmetic Asian call option; we choose a contract with slightly longer maturity (the vanilla option has maturity of 14 months, as opposed to the 12 months term of the Asian option) as to guarantee the hedging position at least until the expiration of the Asian contracts under consideration. Both delta and delta-gamma portfolios are rebalanced at each monitoring date according to the current (re-computed) values of the options' delta and gamma.

Consistently with our observation in Section 4.1, we note from Figure 6 that the hedging errors achieve their lowest level for in-the-money options; both hedging strategies perform poorly for out-of-the-money options, and this is particularly evident for the delta hedge of the out-of-the-money option in the low volatility case (top left corner panel). In this case, in fact, the hedging error can reach up to about 9 times the (forward) option's premium, whilst the one originated by the delta-gamma portfolio is around 12%. However, the delta-gamma strategy always outperforms the delta portfolio by reducing the hedging error on average by more than 70% (we note the scale of the plots in Figure 6). The most significant reduction occurs for high volatility levels; for each volatility value, the improvement of the performance is particularly noticeable in correspondence of the median trajectory. This shows that the introduction of options in the hedging portfolio allows achieving an acceptable performance even in presence of jumps, as it reduces the residual risk and its sensitivity to different scenarios (represented by the different quantile trajectories), in spite of a more conservative option position in the delta-gamma hedge as observed in Section 4.1 in correspondence of high volatility conditions. This feature is in a sense consistent with the market incompleteness caused by discontinuities in asset prices, meant as the impossibility of replicating any option by trading in the underlying asset alone, and the need of 'completing' the market with derivative instruments whose price encapsulates information about the jump risk premium.

4.3   Model error

In order to quantify the error originated by model misspecification, we compare the performance of the delta and delta-gamma hedging portfolios formed using the Asian option's Greeks obtained under the NIG model (model hedging portfolios) with the corresponding

ones constructed using the contract's Greeks computed under the Black–Scholes model, i.e. the case of the Brownian motion with drift (Black–Scholes hedging portfolios). The volatility parameter in the Black–Scholes model is set so that the log-return processes show the same variance under both the Gaussian and the NIG models. In other words we assume that, just after the price of the underlying asset is revealed, the traders re-adjust their position according to the values of the Asian option's Greeks obtained using the Black–Scholes model, due to the fact that they cannot observe directly the actual process originating the underlying asset prices (which in this example is assumed to be the exponential NIG process). The delta-gamma portfolios composition is the same as in the previous section. Results are presented in Figures 7–9, in which we plot the evolution of the hedging errors originated by both the model and the Black–Scholes hedging portfolios over the given contract's term. Due to our construction of the hedging error, we interpret the difference between these hedging errors as model error, as it actually quantifies the difference between the hedging portfolio values obtained under the two model specifications (divided by the forward option's premium, which is assumed to be the same for both models as if directly observed in the market).

We note from the plots that the Black–Scholes delta hedge consistently originates a smaller hedging error than the model delta hedge, especially for high level of volatility of the underlying. The portfolios are however almost undistinguishable along the median trajectories (see Panels 7d–7f, 8d–8f and 9d–9f): over the contract's term, the difference between the hedging errors of the model and the Black–Scholes portfolios, in fact, ranges on average between 0.84% and 1.43% of the (forward) option's premium. In the case of the 'extreme' trajectories, though, these differences can vary between 10% and 67%. These results are consistent with the findings of Denkl et al. (2013).

In any case, the hedging errors are quite significant also under the Black–Scholes model: over the lifetime of the contract, these vary on average between 0.68% to almost 10 times the (forward) option's price when the underlying volatility is set at 10%; the error range narrows to 10%-98% on average for the 30% volatility case, and 9%-95% on average for the 50% volatility case.

Similarly to what observed in the previous section, the delta-gamma portfolios perform

better than the delta ones reducing sensibly the hedging errors; in this case, though, the model delta-gamma hedge performs consistently better than the Black–Scholes one, due to the ability of the relevant sensitivities to adequately capture the impact of potential price shocks. Model error is actually substantial across all strikes, scenarios and volatility levels considered in this analysis, as the difference between the model and the Black–Scholes delta-gamma hedging portfolios varies on average between 22% and around 6 times the option's (forward) premium over the lifetime of the contract. The hedging error originated by the Black–Scholes portfolios, though, reduces in the case of high volatility: as the skewness and excess kurtosis of the NIG distribution are kept constant, the impact of jumps reduces. Hence, the performance of the hedging portfolios obtained under the two alternative modelling assumptions is comparable as the variance is the predominant component requiring accurate quantification.

5   Conclusions

In this paper, we have derived backward integral recursions for the price sensitivities of arithmetic Asian options with discrete monitoring. In particular, we have proved the cases of the option's delta and gamma for an underlying that evolves according to a general exponential Lévy process, and the option's vega for a lognormal underlying; however we note that similar recursive integrals may be obtained for other price sensitivities of practical relevance. Numerical examples show the high accuracy of the proposed approach across different distribution laws for the log-returns, parameter values, strike prices and sensitivity types.

The price sensitivities have been then used to assess both the performance of Greeks-based hedging strategies in an incomplete market, and the impact of model error. We find that the delta-gamma hedge is superior to the delta hedge in terms of reduction of the risk exposure; further incorrectly specifying the underlying price dynamics leads to non-trivial error which can be significant especially in the case of the delta-gamma hedge.

The presence of jumps in the dynamics of the underlying asset, the inclusion of the delta-gamma portfolio and the study of the hedging error and model error distinguish our paper

from earlier contributions by Jacques (1996) and Yang et al. (2011). Future research is directed at extending the analysis by comparing the quadratic hedging strategies of Cont et al. (2007) with the delta-gamma hedge and assessing the hedging error under different market conditions in terms of volatility, skewness and excess kurtosis.

Acknowledgements

Appendix A   Proof of Theorem 1

Proof of (i).   The proof proceeds by backward induction on k. For $k = n$, we have from (5) that $0 \leq \frac{\partial}{\partial S_0} p_n(y; S_0) = e^y 1_{y > \ln(-\lambda_0)} \leq e^y$. Therefore, $\frac{\partial}{\partial S_0} p_n(y; S_0)$ is dominated by an integrable function over compact intervals and from (6) we get that

$$\frac{\partial}{\partial S_0} \tilde{p}_{n-1}(x; S_0) = \int_{-\infty}^{\infty} \frac{\partial}{\partial S_0} p_n(x + z; S_0) f_n(z) dz, \tag{A.1}$$

which is non-negative. Further,

$$\frac{\partial}{\partial S_0} \tilde{p}_{n-1}(x; S_0) \leq \int_{-\infty}^{\infty} e^{x+z} f_n(z) dz = \mu_n e^x = \alpha_n + \beta_{n-1} e^x.$$

It follows from (7) that

$$0 \leq \frac{\partial}{\partial S_0} p_{n-1}(y; S_0) \leq \alpha_n + \beta_{n-1} \lambda_1 + \beta_{n-1} e^y = \alpha_{n-1} + \beta_{n-1} e^y.$$

Now suppose that (14) holds for arbitrary $k < n$. Then the function $\frac{\partial}{\partial S_0} p_k(y; S_0) \geq 0$ is integrable over compact intervals. As $f_k \geq 0$, we get

$$
\begin{aligned}
0 \;\leq\; & \frac{\partial}{\partial S_0} \tilde{p}_{k-1}(x; S_0) = \int_{-\infty}^{\infty} \frac{\partial}{\partial S_0} p_k(x + z; S_0) f_k(z) dz \tag{A.2} \\
\leq\; & \int_{-\infty}^{\infty} (\alpha_k + \beta_k e^{x+z}) f_k(z) dz = \alpha_k + \beta_{k-1} e^x
\end{aligned}
$$

and

$$
0 \leq \frac{\partial}{\partial S_0} p_{k-1}(y; S_0) \leq \alpha_k + \beta_{k-1} \lambda_{n+1-k} + \beta_{k-1} e^x = \alpha_{k-1} + \beta_{k-1} e^y.
$$

∎

Proof of (ii). From (A.1), $\frac{\partial^2}{\partial S_0^2} \tilde{p}_{n-1}(x; S_0)$ is well-defined and is given by

$$
\frac{\partial^2}{\partial S_0^2} \tilde{p}_{n-1}(x; S_0) = -\frac{\lambda_0}{S_0} f_n(-x + \ln(-\lambda_0)) \geq 0.
$$

In addition, from (7)

$$
\frac{\partial^2}{\partial S_0^2} p_{n-1}(y; S_0) = -\frac{\lambda_0}{S_0} f_n(- \ln(e^y + \lambda_1) + \ln(-\lambda_0)) \geq 0,
$$

so that

$$
\int_L^U \frac{\partial^2}{\partial S_0^2} p_{n-1}(y; S_0) dy = -\frac{\lambda_0}{S_0} \int_L^U f_n \left(\ln \left(-\frac{\lambda_0}{e^y + \lambda_1} \right) \right) dy = -\frac{\lambda_0}{S_0} \int_{L'}^{U'} \frac{1}{1 + \lambda_1 e^w / \lambda_0} f_n(w) dw,
$$

where $L' := \ln(-\lambda_0 / (\lambda_1 + e^U))$ and $U' := \ln(-\lambda_0 / (\lambda_1 + e^L))$. As $w \leq U'$, $\lambda_0 < 0$ and $\lambda_1 > 0$, it follows that $1/(1 + \lambda_1 e^w / \lambda_0) \leq 1 + \lambda_1 e^{-L}$ and

$$
\begin{aligned}
\int_L^U \frac{\partial^2}{\partial S_0^2} p_{n-1}(y; S_0) dy \;\leq\; & -\frac{\lambda_0 (1 + \lambda_1 e^{-L})}{S_0} \int_{L'}^{U'} f_n(w) dw \\
\leq\; & -\frac{\lambda_0 (1 + \lambda_1 e^{-L})}{S_0} = \gamma_{n-1} + \varepsilon_{n-1} e^{-L},
\end{aligned}
$$

which is finite for finite L. Hence, the statement is true for $k = n - 1$. Now suppose the statement is true for arbitrary $k < n - 1$. Therefore the function $\frac{\partial^2}{\partial S_0^2} p_k(y; S_0) \geq 0$ is

integrable for y in a compact interval, and from (A.2) we get

$$0 \leq \frac{\partial^2}{\partial S_0^2} \tilde{p}_{k-1}(x; S_0) = \int_{-\infty}^{\infty} \frac{\partial^2}{\partial S_0^2} p_k(x + z; S_0) f_k(z) dz$$

and from (7)

$$0 \leq \frac{\partial^2}{\partial S_0^2} p_{k-1}(y; S_0) = \frac{\partial^2}{\partial S_0^2} \tilde{p}_{k-1}(\ln(e^y + \lambda_{n+1-k}); S_0).$$

Then,

$$
\begin{aligned}
\int_L^U \frac{\partial^2}{\partial S_0^2} p_{k-1}(y; S_0) dy &= \int_L^U \int_{-\infty}^{\infty} \frac{\partial^2}{\partial S_0^2} p_k(\ln(e^y + \lambda_{n+1-k}) + z; S_0) f_k(z) dz dy \\
&= \int_{-\infty}^{\infty} f_k(z) \int_{z+\ln(e^L+\lambda_{n+1-k})}^{z+\ln(e^U+\lambda_{n+1-k})} \frac{\partial^2}{\partial S_0^2} p_k(w; S_0) \frac{1}{1 - \lambda_{n+1-k} e^{z-w}} dw dz.
\end{aligned}
$$

As $w \geq z + \ln(e^L + \lambda_{n+1-k})$ and $\lambda_{n+1-k} > 0$ for $k < n-1$, we have that $1/(1 - \lambda_{n+1-k} e^{z-w}) \leq 1 + \lambda_{n+1-k} e^{-L}$ leading to

$$
\begin{aligned}
\int_L^U \frac{\partial^2}{\partial S_0^2} p_{k-1}(y; S_0) dy &\leq (1 + \lambda_{n+1-k} e^{-L}) \int_{-\infty}^{\infty} f_k(z) \int_{z+\ln(e^L+\lambda_{n+1-k})}^{z+\ln(e^U+\lambda_{n+1-k})} \frac{\partial^2}{\partial S_0^2} p_k(w; S_0) dw dz \\
&\leq (1 + \lambda_{n+1-k} e^{-L}) \int_{-\infty}^{\infty} \left(\gamma_k + \varepsilon_k \frac{e^{-z}}{e^L + \lambda_{n+1-k}} \right. \\
&\quad \left. + \zeta_k e^z (e^U + \lambda_{n+1-k}) + \eta_k \frac{e^U + \lambda_{n+1-k}}{e^L + \lambda_{n+1-k}} \right) f_k(z) dz,
\end{aligned}
$$

which is finite for finite L, U. Result (15) follows by straightforward integration. ■

Proof of (iii). Follows from the proofs of parts (i)–(ii) of the Theorem. This concludes the proof of the Theorem. ■

Appendix B   Mathematical analysis towards proving Theorem 2

We begin the path to proving Theorem 2 by providing some necessary results.

Lemma 3 *There exists sequence of positive constants given by*

$$A_n = S_0, \ A_k = A_{k+1}(e^{-(r-\sigma^2)\delta} + e^{r\delta})(1 + \lambda_{n-k}),$$

such that

$$p_k(y) \leq A_k e^{|y|} \text{ for } k \leq n,$$

$$\tilde{p}_k(x) \leq A_{k+1}(e^{-(r-\sigma^2)\delta} + e^{r\delta})e^{|x|} \text{ for } k < n,$$

for all y and x.

Proof. From (5) we have that $p_n(y) \leq S_0 e^{|y|}$. The proof proceeds by induction. Assume that $p_k(y) \leq A_k e^{|y|}$ holds for arbitrary $k < n$. Then from (6)

$$\tilde{p}_{k-1}(x) \leq A_k \left(\int_{-\infty}^{-x} e^{-x-z} f(z)\, dz + \int_{-x}^{\infty} e^{x+z} f(z)\, dz \right),$$

where

$$f(z) = \frac{1}{\sigma\sqrt{\delta}} \phi\left(\frac{z - (r - \frac{1}{2}\sigma^2)\delta}{\sigma\sqrt{\delta}} \right)$$

and ϕ is the standard normal density function. Using the substitution $w := (z - (r - \frac{1}{2}\sigma^2)\delta)/(\sigma\sqrt{\delta})$ and for $w_0(x) := (-x - (r - \frac{1}{2}\sigma^2)\delta)/(\sigma\sqrt{\delta})$, we get

$$
\begin{aligned}
\tilde{p}_{k-1}(x) &\leq A_k \left(\int_{-\infty}^{w_0(x)} e^{-x-w\sigma\sqrt{\delta}-(r-\frac{1}{2}\sigma^2)\delta} \phi(w)\, dw + \int_{w_0(x)}^{\infty} e^{x+w\sigma\sqrt{\delta}+(r-\frac{1}{2}\sigma^2)\delta} \phi(w)\, dw \right) \\
&= A_k \left[e^{-x-(r-\sigma^2)\delta} \Phi\left(w_0(x) + \sigma\sqrt{\delta} \right) + e^{x+r\delta}\left(1 - \Phi\left(w_0(x) - \sigma\sqrt{\delta} \right) \right) \right] \\
&\leq A_k(e^{-(r-\sigma^2)\delta} + e^{r\delta})e^{|x|},
\end{aligned}
$$

where Φ denotes the standard normal cumulative distribution function, and, from (7),

$$
\begin{aligned}
p_{k-1}(y) &\leq A_k(e^{-(r-\sigma^2)\delta} + e^{r\delta}) \max\left(e^y + \lambda_{n+1-k}, \frac{1}{e^y + \lambda_{n+1-k}} \right) \\
&\leq A_k(e^{-(r-\sigma^2)\delta} + e^{r\delta})(1 + \lambda_{n+1-k})e^{|y|} = A_{k-1}e^{|y|}.
\end{aligned}
$$

∎

Corollary 4 $\lim_{w \to \pm\infty} p_k(x + w\sigma\sqrt{\delta} + (r - \frac{1}{2}\sigma^2)\delta)w\phi(w) = 0.$

Proof. Follows from Lemma 3. ∎

Lemma 5 *There exists sequence of positive constants given by*

$$B_k = S_0(e^{-(r-\sigma^2)\delta} + e^{r\delta})^{n-k},$$

such that

$$p'_k(y) \leq B_k e^{|y|} \text{ for } k \leq n,$$

$$\tilde{p}'_k(x) \leq B_k e^{|x|} \text{ for } k < n,$$

for all y and x.

Proof. We have that $p'_n(y) \leq S_0 e^{|y|}$. Assume that $p'_k(y) \leq B_k e^{|y|}$ for arbitrary $k < n$. Then the proof of $\tilde{p}'_{k-1}(x) \leq B_k(e^{-(r-\sigma^2)\delta} + e^{r\delta})e^{|x|}$ is identical to that of $\tilde{p}_{k-1}$ in Lemma 3. Then, from (7)

$$
\begin{aligned}
p'_{k-1}(y) &= \tilde{p}'_{k-1}(h_{k-1}(y))h'_{k-1}(y) \\
&\leq \frac{B_k(e^{-(r-\sigma^2)\delta} + e^{r\delta})e^y}{\lambda_{n+1-k} + e^y} \max\left(\lambda_{n+1-k} + e^y, \frac{1}{\lambda_{n+1-k} + e^y}\right) \\
&= B_k(e^{-(r-\sigma^2)\delta} + e^{r\delta}) \max\left(e^y, \frac{e^y}{(\lambda_{n+1-k} + e^y)^2}\right) \\
&\leq B_k(e^{-(r-\sigma^2)\delta} + e^{r\delta})e^{|y|} = B_{k-1}e^{|y|}.
\end{aligned}
$$

∎

Corollary 6 $\lim_{w\to\pm\infty} p'_k(x + w\sigma\sqrt{\delta} + (r - \frac{1}{2}\sigma^2)\delta)\phi(w) = 0.$

Proof. Follows from Lemma 5. ∎

Lemma 7 *For $k \leq n - 1$,*

$$0 \leq \tilde{p}''_k(x) - \tilde{p}'_k(x) \leq C_k e^x, \tag{B.1}$$

$$0 \leq p''_k(y) - p'_k(y) \leq C_k e^y \tag{B.2}$$

for all x and y, where $C_k = \frac{1}{\sigma\sqrt{2\pi\delta}} S_0 e^{r\delta(n-k)}.$

Proof. We have that

$$p'_k(y) = \tilde{p}'_k(h_k(y))h'_k(y) = \frac{e^y}{e^y + \lambda_{n-k}}\tilde{p}'_k(h_k(y))$$

and

$$p''_k(y) = \frac{\lambda_{n-k}e^y}{(e^y + \lambda_{n-k})^2}\tilde{p}'_k(h_k(y)) + \left(\frac{e^y}{e^y + \lambda_{n-k}}\right)^2 \tilde{p}''_k(h_k(y)),$$

hence

$$p''_k(y) - p'_k(y) = \left(\frac{e^y}{e^y + \lambda_{n-k}}\right)^2 (\tilde{p}''_k(h_k(y)) - \tilde{p}'_k(h_k(y))).$$

If (B.1) holds, then

$$0 \le p''_k(y) - p'_k(y) \le \left(\frac{e^y}{e^y + \lambda_{n-k}}\right)^2 C_k(e^y + \lambda_{n-k}) \le C_k e^y$$

and (B.2) holds as well. Consider the case $k = n - 1$. Under the assumptions of the Black–Scholes framework, (6) solves explicitly to

$$\tilde{p}_{n-1}(x) = S_0 e^{x+r\delta}\Phi\left(\frac{x - \ln(-\lambda_0) + (r + \frac{1}{2}\sigma^2)\delta}{\sigma\sqrt{\delta}}\right) + \lambda_0 S_0 \Phi\left(\frac{x - \ln(-\lambda_0) + (r - \frac{1}{2}\sigma^2)\delta}{\sigma\sqrt{\delta}}\right). \tag{B.3}$$

We then get

$$\tilde{p}'_{n-1}(x) = S_0 e^{x+r\delta}\Phi\left(\frac{x - \ln(-\lambda_0) + (r + \frac{1}{2}\sigma^2)\delta}{\sigma\sqrt{\delta}}\right),$$

$$\tilde{p}''_{n-1}(x) = \tilde{p}'_{n-1}(x) + \frac{1}{\sigma\sqrt{\delta}}S_0 e^{x+r\delta}\phi\left(\frac{x - \ln(-\lambda_0) + (r + \frac{1}{2}\sigma^2)\delta}{\sigma\sqrt{\delta}}\right),$$

from which it is evident that (B.1) and, hence, (B.2) hold for $k = n - 1$. The remainder of the proof proceeds by induction: if (B.1), (B.2) hold for arbitrary k, then

$$\tilde{p}''_{k-1}(x) - \tilde{p}'_{k-1}(x) = \int_{-\infty}^{\infty} (p''_k(x + z) - p'_k(x + z))f(z)\,dz$$

obtained from (6) is well-defined and

$$0 \le \tilde{p}''_{k-1}(x) - \tilde{p}'_{k-1}(x) \le \int_{-\infty}^{\infty} C_k e^{x+z} f(z)\,dz = C_k e^{r\delta}e^x = C_{k-1}e^x.$$

This completes the proof of the Lemma. ∎

B.1 Proof of Theorem 2

Proof of (i). From (B.3) we get

$$
\begin{aligned}
\frac{\partial}{\partial\sigma}\tilde{p}_{n-1}(x;\sigma) &= S_0\sqrt{\delta}e^{x+r\delta}\phi\left(\frac{x-\ln(-\lambda_0)+(r+\frac{1}{2}\sigma^2)\delta}{\sigma\sqrt{\delta}}\right) \le \frac{1}{\sqrt{2\pi}}S_0\sqrt{\delta}e^{r\delta}e^x \\
&= \tilde{c}_{n-1}+d_{n-1}e^x,
\end{aligned}
$$

while

$$
\frac{\partial}{\partial\sigma}p_{n-1}(y;\sigma) = \frac{\partial}{\partial\sigma}\tilde{p}_{n-1}(h_{n-1}(y);\sigma) \le c_{n-1}+d_{n-1}e^y
$$

follows from (7). Clearly $\frac{\partial}{\partial\sigma}\tilde{p}_{n-1}, \frac{\partial}{\partial\sigma}p_{n-1} \ge 0$. The remainder of the proof proceeds by induction. Define

$$
F_{k-1}(x;\sigma) = \int_{-\infty}^{\infty}\left(\frac{\partial}{\partial\sigma}p_k(x+z;\sigma)f(z;\sigma)+p_k(x+z;\sigma)\frac{\partial}{\partial\sigma}f(z;\sigma)\right)dz
$$

for $k \le n-1$. Observe that, as $\phi'(z) = -z\phi(z)$,

$$
\frac{\partial}{\partial\sigma}f(z;\sigma) = \frac{1}{\sigma}\left(\left(\frac{z-(r-\frac{1}{2}\sigma^2)\delta}{\sigma\sqrt{\delta}}\right)^2 - z + \left(r-\frac{1}{2}\sigma^2\right)\delta - 1\right)f(z;\sigma),
$$

hence

$$
\begin{aligned}
F_{k-1}&(x;\sigma) = \\
&\int_{-\infty}^{\infty}\left[\frac{\partial}{\partial\sigma}p_k(x+z;\sigma)+\frac{1}{\sigma}\left(\left(\frac{z-(r-\frac{1}{2}\sigma^2)\delta}{\sigma\sqrt{\delta}}\right)^2 - z + \left(r-\frac{1}{2}\sigma^2\right)\delta - 1\right)p_k(x+z;\sigma)\right]f(z;\sigma)dz.
\end{aligned}
$$

Using the substitution $w := (z - (r - \frac{1}{2}\sigma^2)\delta)/(\sigma\sqrt{\delta})$ and for $z(w) = w\sigma\sqrt{\delta} + (r - \frac{1}{2}\sigma^2)\delta$, we obtain further

$$F_{k-1}(x;\sigma) =$$
$$\int_{-\infty}^{\infty} \left[\frac{\partial}{\partial\sigma}p_k(x + z(w);\sigma) + \frac{1}{\sigma}(w^2 - w\sigma\sqrt{\delta} - 1)p_k(x + z(w);\sigma)\right]\phi(w)dw = \quad \text{(B.4)}$$
$$\int_{-\infty}^{\infty} \left[\frac{\partial}{\partial\sigma}p_k(x + z(w);\sigma) + \frac{1}{\sigma}\left(\left(w - \frac{1}{2}\sigma\sqrt{\delta}\right)^2 - \frac{1}{4}\sigma^2\delta - 1\right)p_k(x + z(w);\sigma)\right]\phi(w)dw.$$

Assume that (17) holds for arbitrary $k \leq n - 1$. In addition, from (9) we have $0 \leq p_k(y) \leq a_k + b_k e^y$ for all k. Then,

$$\begin{aligned}
F_{k-1}(x;\sigma) &\leq \int_{-\infty}^{\infty} \left[\frac{\partial}{\partial\sigma}p_k(x + z(w);\sigma) + \frac{1}{\sigma}\left(w - \frac{1}{2}\sigma\sqrt{\delta}\right)^2 p_k(x + z(w);\sigma)\right]\phi(w)dw \\
&\leq \int_{-\infty}^{\infty} \left[c_k + d_k e^{x+z(w)} + \frac{1}{\sigma}\left(w - \frac{1}{2}\sigma\sqrt{\delta}\right)^2 (a_k + b_k e^{x+z(w)})\right]\phi(w)dw \\
&= c_k + a_k\left(\frac{1}{\sigma} + \frac{1}{4}\sigma\delta\right) + \left(d_k + b_k\left(\frac{1}{\sigma} + \frac{1}{4}\sigma\delta\right)\right)e^{r\delta}e^x = \tilde{c}_{k-1} + d_{k-1}e^x,
\end{aligned}$$

hence $F_{k-1}(x;\sigma)$ is finite for x in a compact interval. Then, in differentiating (6) with respect to σ, it is implied that

$$F_{k-1}(x;\sigma) = \frac{\partial}{\partial\sigma}\tilde{p}_{k-1}(x;\sigma) \leq \tilde{c}_{k-1} + d_{k-1}e^x \quad \text{(B.5)}$$

and from (7)

$$\frac{\partial}{\partial\sigma}p_{k-1}(y;\sigma) = \frac{\partial}{\partial\sigma}\tilde{p}_{k-1}(h_{k-1}(y);\sigma) \leq c_{k-1} + d_{k-1}e^y.$$

Next we prove that $\frac{\partial}{\partial\sigma}\tilde{p}_{k-1}, \frac{\partial}{\partial\sigma}p_{k-1} \geq 0$ for arbitrary k. To this end, consider two preliminary results. First, by integration by parts we get

$$\begin{aligned}
\int_{-\infty}^{\infty} w^2 p_k(x + z(w);\sigma)\phi(w)dw &= [-w p_k(x + z(w);\sigma)\phi(w)]_{-\infty}^{\infty} \\
&+ \int_{-\infty}^{\infty} (p_k(x + z(w);\sigma) + w z'(w)\partial_1 p_k(x + z(w);\sigma))\phi(w)dw,
\end{aligned}$$

where the first term on the right hand side is zero by Corollary 4.[2] Hence,

$$\int_{-\infty}^{\infty} (w^2 - 1)p_k(x + z(w); \sigma)\phi(w)dw = \int_{-\infty}^{\infty} w\sigma\sqrt{\delta}\partial_1 p_k(x + z(w); \sigma)\phi(w)dw. \qquad (B.6)$$

Second, for any function H we have

$$\int_{-\infty}^{\infty} wH(z(w))\phi(w)dw = [-H(z(w))\phi(w)]_{-\infty}^{\infty} + \int_{-\infty}^{\infty} H'(z(w))z'(w)\phi(w)dw; \qquad (B.7)$$

note that for $H := \partial_1 p_k - p_k$ and based on Corollaries 4 and 6, the first term on the right hand side of (B.7) is zero. From (B.4), (B.5), (B.6), (B.7), we get

$$\begin{aligned}
&\frac{\partial}{\partial\sigma}\tilde{p}_{k-1}(x; \sigma) \\
&= \int_{-\infty}^{\infty} \left[\frac{\partial}{\partial\sigma}p_k(x + z(w); \sigma) + \sigma\delta(\partial_{11}p_k(x + z(w); \sigma) - \partial_1 p_k(x + z(w); \sigma))\right]\phi(w)dw \\
&\geq 0
\end{aligned}$$

as a consequence of Lemma 7. Also, $\frac{\partial}{\partial\sigma}p_{k-1}(y; \sigma) = \frac{\partial}{\partial\sigma}\tilde{p}_{k-1}(h_{k-1}(y); \sigma) \geq 0$. ∎

Proof of (ii). Follows from the proof of part (i) of the Theorem. This concludes the proof of the Theorem. ∎

References

Andricopoulos, A.D., Widdicks, M., Duck, P.W., Newton, D.P. (2003). Universal option valuation using quadrature methods. Journal of Financial Economics 67, 447–471.

Ballotta, L., Kyriakou, I. (2014). Monte Carlo simulation of the CGMY process and option pricing. Journal of Futures Markets 34, 1095–1121.

Barndorff-Nielsen, O.E. (1995). Normal inverse Gaussian distributions and the modeling of stock returns. Technical Report Research report No. 300. Department of Theoretical Statistics, Aarhus University. Aarhus, Denmark.

---

[2]We use $\partial_1 p$ (resp. $\partial_{11}p$) to denote the first (resp. second) partial derivative of p with respect to its first argument.

Bayazit, D., Nolder, C.A. (2013). Sensitivities of options via Malliavin calculus: applications to markets of exponential Variance Gamma and Normal Inverse Gaussian processes. Quantitative Finance 13, 1257–1287.

Bluestein, L.I. (1968). A linear filtering approach to the computation of the discrete Fourier transform. IEEE Northeast Electronics Research and Engineering Meeting 10, 218–219.

Broadie, M., Glasserman, P. (1996). Estimating security price derivatives using simulation. Management Science 42, 269–285.

Brodén, M., Tankov, P. (2011). Tracking errors from discrete hedging in exponential Lévy models. International Journal of Theoretical and Applied Finance 14, 803–837.

Carr, P., Ewald, C.O., Xiao, Y. (2008). On the qualitative effect of volatility and duration on prices of Asian options. Finance Research Letters 5, 162–171.

Carr, P., Geman, H., Madan, D.B., Yor, M. (2002). The fine structure of asset returns: an empirical investigation. Journal of Business 75, 305–332.

Carr, P., Madan, D.B. (1999). Option valuation using the fast Fourier transform. Journal of Computational Finance 2, 61–73.

Carverhill, A., Clewlow, L. (1990). Flexible convolution. Risk 3, 25–29.

Černý, A. (2004). Introduction to Fast Fourier Transform in Finance. Journal of Derivatives 12, 73–88.

Černý, A., Kyriakou, I. (2011). An improved convolution algorithm for discretely sampled Asian options. Quantitative Finance 11, 381–389.

Cont, R., Tankov, P., Voltchkova, E. (2007). Hedging with options in models with jumps, in: Stochastic Analysis and Applications – the Abel Symposium 2005. Springer.

Corcuera, J.M., Guillaume, F., Leoni, P., Schoutens, W. (2008). Implied Lévy volatility. Technical Report TR-08-07. Department of Mathematics, University of Leuven. Leuven, Belgium.

Corsaro, S., Marazzina, D., Marino, Z. (2015). A parallel wavelet-based pricing procedure for Asian options. Quantitative Finance 15, 101–113.

Curran, M. (1994). Strata Gems. Risk 7, 70–71.

Curran, M. (1998). Greeks in Monte Carlo, in: Dupire, B. (Ed.), Monte Carlo Methodologies and Applications for Pricing and Risk Management. Risk Books, London.

Denkl, S., Goy, M., Kallsen, J., Muhle-Karbe, J., Pauwels, A. (2013). On the performance of delta-hedging strategies in exponential Lévy models. Quantitative Finance 13, 1173–1184.

Eberlein, E., Papapantoleon, A. (2005). Equivalence of floating and fixed strike Asian and lookback options. Stochastic Processes and their Applications 115, 31–40.

Fusai, G., Marazzina, D., Marena, M. (2011). Pricing discretely monitored Asian options by maturity randomization. SIAM Journal on Financial Mathematics 2, 383–403.

Fusai, G., Marena, M., Roncoroni, A. (2008). Analytical pricing of discretely monitored Asian-style options: Theory and application to commodity markets. Journal of Banking and Finance 32, 2033–2045.

Fusai, G., Meucci, A. (2008). Pricing discretely monitored Asian options under Lévy processes. Journal of Banking and Finance 32, 2076–2088.

Garman, M. (1992). Charm School. Risk 5, 53–56.

Glasserman, P. (2004). Monte Carlo Methods in Financial Engineering. Springer, New York.

Glasserman, P., Liu, Z. (2010). Sensitivity estimates from characteristic functions. Operations Research 58, 1611–1623.

Gobet, E., Makhlouf, A. (2012). The tracking error rate of delta-gamma hedging strategy. Mathematical Finance 22, 277–309.

Goutte, S., Oudjane, N., Russo, F. (2013). Variance-optimal hedging for discrete-time processes with independent increments: application to electricity markets. Journal of Computational Finance 17, 71–111.

Goutte, S., Oudjane, N., Russo, F. (2014). Variance optimal hedging for continuous time additive processes and applications. Stochastics: An International Journal of Probability and Stochastic Processes 86, 147–185.

Jacques, M. (1996). On the hedging portfolios of Asian options. ASTIN Bulletin 26, 165–183.

Lo, K.H., Wang, K., Hsu, M.F. (2008). Pricing European Asian options with skewness and kurtosis in the underlying distribution. Journal of Futures Markets 28, 598–616.

Marena, M., Roncoroni, A., Fusai, G. (2013). Asian options with jumps. Argo Newsletter – New Frontiers in Practical Risk Management 1, 47–56.

Nomikos, N.K., Kyriakou, I., Papapostolou, N.C., Pouliasis, P.K. (2013). Freight options: Price modelling and empirical analysis. Transportation Research Part E: Logistics and Transportation Review 51, 82–94.

Rabiner, L.R., Schafer, R.W., Rader, C.M. (1969). The chirp z-transform algorithm and its application. Bell System Technical Journal 48, 1249–1292.

Tankov, P. (2010). Pricing and hedging in exponential Lévy models: Review of recent results, in: Paris-Princeton Lecture Notes in Mathematical Finance. Springer.

Večeř, J. (2002). Unified Asian pricing. Risk 15, 113–116.

Webb, A. (1999). The sensitivity of Vega. Derivatives Strategy November, 16–19.

de Weert, F. (2008). Exotic Options Trading. Wiley Finance Series, John Wiley & Sons.

Yang, Z., Ewald, C.O., Menkens, O. (2011). Pricing and hedging of Asian options: quasi-explicit solutions via Malliavin calculus. Mathematical Methods of Operations Research 74, 93–120.

Zhang, B., Oosterlee, C.W. (2013). Efficient pricing of European-style Asian options under exponential Lévy processes based on Fourier cosine expansions. SIAM Journal on Financial Mathematics 4, 399–426.

Table 1

(a) Risk neutral model parameters.

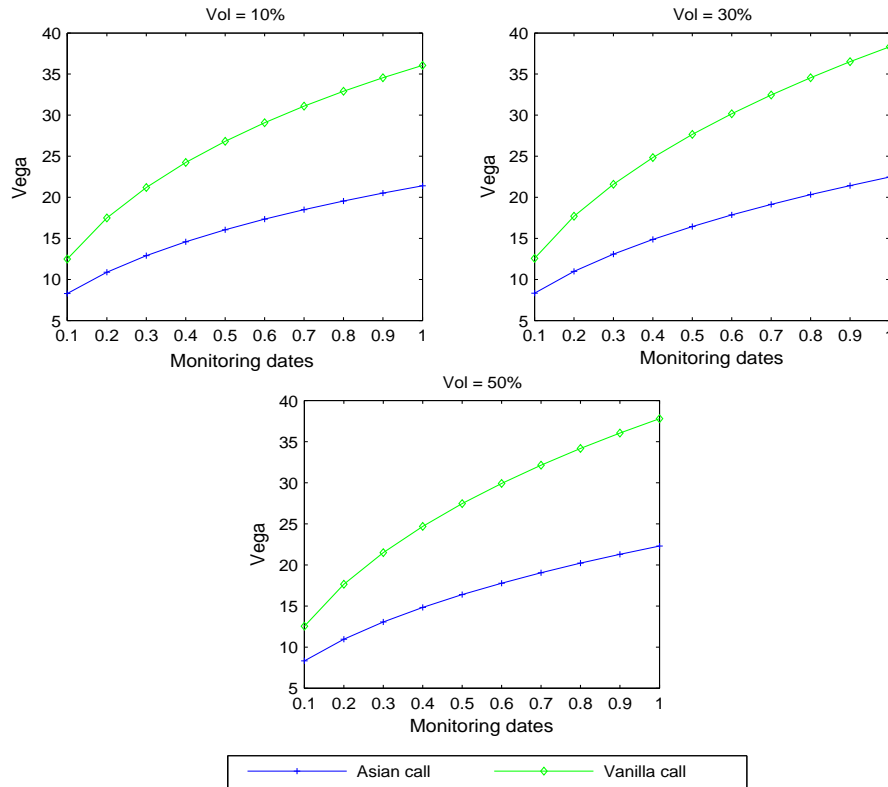| BS	CGMY				NIG		
σ	C	G	M	Y	ν	γ	θ
0.1	0.2703	17.56	54.82	0.8	0.1222	0.0879	−0.1364
0.3	0.6509	5.853	18.27	0.8	0.1222	0.2637	−0.4091
0.5	0.9795	3.512	10.96	0.8	0.1222	0.4395	−0.6819

(b) Arithmetic Asian call option price sensitivities.

model	Vol	K 90	K 100	K 110	K 90		K 100		K 110	
		Delta recursion			CVMC PW Delta (std. error $\times 10^{-5}$)					
BS	0.1	0.966536	0.632629	0.105740	0.9665	(9)	0.6325	(17)	0.1059	(22)
	0.3	0.770593	0.563355	0.356690	0.7706	(28)	0.5628	(30)	0.3569	(34)
	0.5	0.695404	0.563825	0.438759	0.6958	(38)	0.5637	(40)	0.4391	(44)
NIG	0.1	0.956400	0.671022	0.080918	0.9564	(11)	0.6711	(17)	0.0809	(21)
	0.3	0.799574	0.598537	0.362400	0.7994	(28)	0.5979	(29)	0.3623	(33)
	0.5	0.731009	0.592983	0.448609	0.7306	(37)	0.5926	(38)	0.4484	(40)
CGMY	0.1	0.956498	0.670591	0.081181	0.9567	(11)	0.6707	(17)	0.0813	(21)
	0.3	0.799228	0.598308	0.362797	0.7991	(28)	0.5977	(29)	0.3631	(33)
	0.5	0.730686	0.592920	0.448945	0.7305	(37)	0.5929	(38)	0.4485	(40)
		Gamma recursion			CVMC LRPW Gamma (std. error $\times 10^{-5}$)					
BS	0.1	0.0062364	0.0622252	0.0304433	0.00625	(6)	0.06226	(13)	0.03043	(15)
	0.3	0.0165627	0.0218205	0.0205350	0.01651	(6.5)	0.02199	(7.5)	0.02051	(8)
	0.5	0.0116627	0.0130656	0.0129548	0.01161	(5.3)	0.01297	(5.8)	0.01293	(6)
NIG	0.1	0.0065512	0.0596221	0.0313875	0.00659	(15)	0.05947	(25)	0.03135	(33)
	0.3	0.0144623	0.0232580	0.0246266	0.01432	(14)	0.02319	(16)	0.02482	(17)
	0.5	0.0114808	0.0144927	0.0154340	0.01166	(12)	0.01460	(12)	0.01553	(13)
CGMY	0.1	0.0065464	0.0596070	0.0315333	0.00669	(15)	0.05953	(27)	0.03168	(34)
	0.3	0.0144825	0.0232080	0.0245690	0.01437	(15)	0.02321	(16)	0.02467	(18)
	0.5	0.0114704	0.0144549	0.0153935	0.01150	(12)	0.01465	(13)	0.01548	(13)
		Vega recursion			CVMC PW Vega (std. error $\times 10^{-3}$)					
BS	0.1	2.060207	21.404443	10.847111	2.068	(12)	21.410	(5.3)	10.864	(17)
	0.3	16.373056	22.460832	21.894896	16.387	(19)	22.475	(12)	21.903	(12)
	0.5	19.118652	22.302081	22.905267	19.091	(28)	22.266	(23)	22.914	(21)

[a] Panel (a) of Table 1 reports the risk neutral model parameters; Panel (b) the arithmetic Asian call option price sensitivities. Results are obtained using backward recursions and control variate Monte Carlo (CVMC) simulations with 100,000 trials (standard errors given in parentheses) for the BS, NIG, CGMY models, one-year log-return volatilities Vol $= \{0.1, 0.3, 0.5\}$ and strike prices $K = \{90, 100, 110\}$. Other parameters: $S_0 = 100$, $r = 0.04$, $T = 1$, $n = 50$.
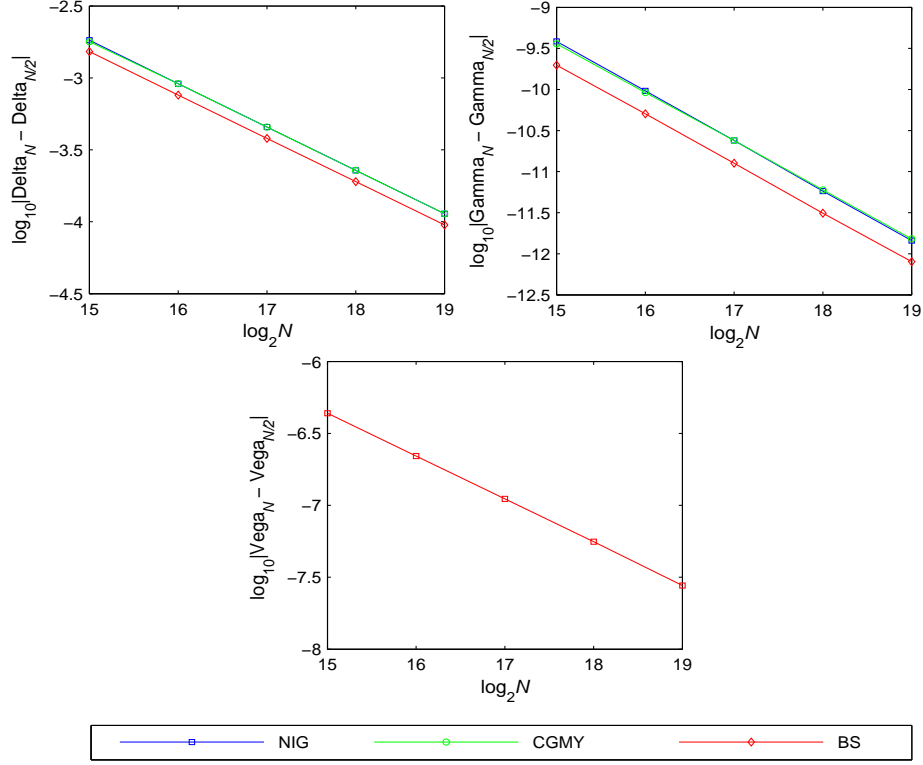
Figure 1
Vega: Asian call vs. plain vanilla call option. Black–Scholes model.

[a] Asian call and plain vanilla call option vega comparison in the Black–Scholes model. Vegas computed, respectively, using our backward recursion for the Asian option and the closed-form expression for the plain vanilla option. Plain vanilla option maturities coincide with the reset dates of the Asian option. One-year log-return volatilities Vol $= \{0.1, 0.3, 0.5\}$. Other parameters: $S_0 = K = 100$, $r = 0.04$, $T = 1$, $n = 50$.
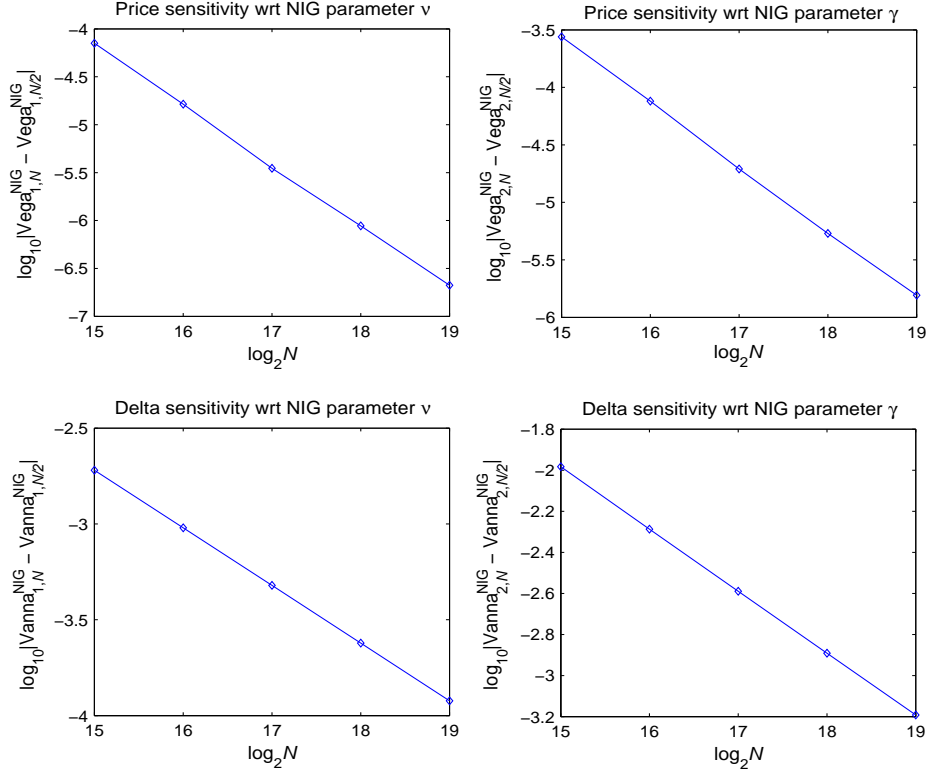
Figure 2

Convergence patterns of computed deltas, gammas and vegas by backward recursion.

^{a} Convergence patterns of numerically computed by backward recursion deltas and gammas (NIG, CGMY, BS models) and vegas (BS model) for an at-the-money Asian call option ($S_0 = K = 100$) and the case of one-year log-return volatility Vol $= 0.1$ (see Panel (a) of Table 1). Delta$_N$, Gamma$_N$, Vega$_N$ denote the relevant sensitivities calculated by numerical implementation of the backward recursive integrals (16) and (18) by discrete Fourier transform (see Černý and Kyriakou, 2011, Section 4) for N discretization points. $|$Delta$_N -$ Delta$_{N/2}|$, $|$Gamma$_N -$ Gamma$_{N/2}|$, $|$Vega$_N -$ Vega$_{N/2}|$ are the absolute differences calculated for $N = 2^{15}, \ldots, 2^{19}$. Other parameters: $r = 0.04$, $T = 1$, $n = 50$.
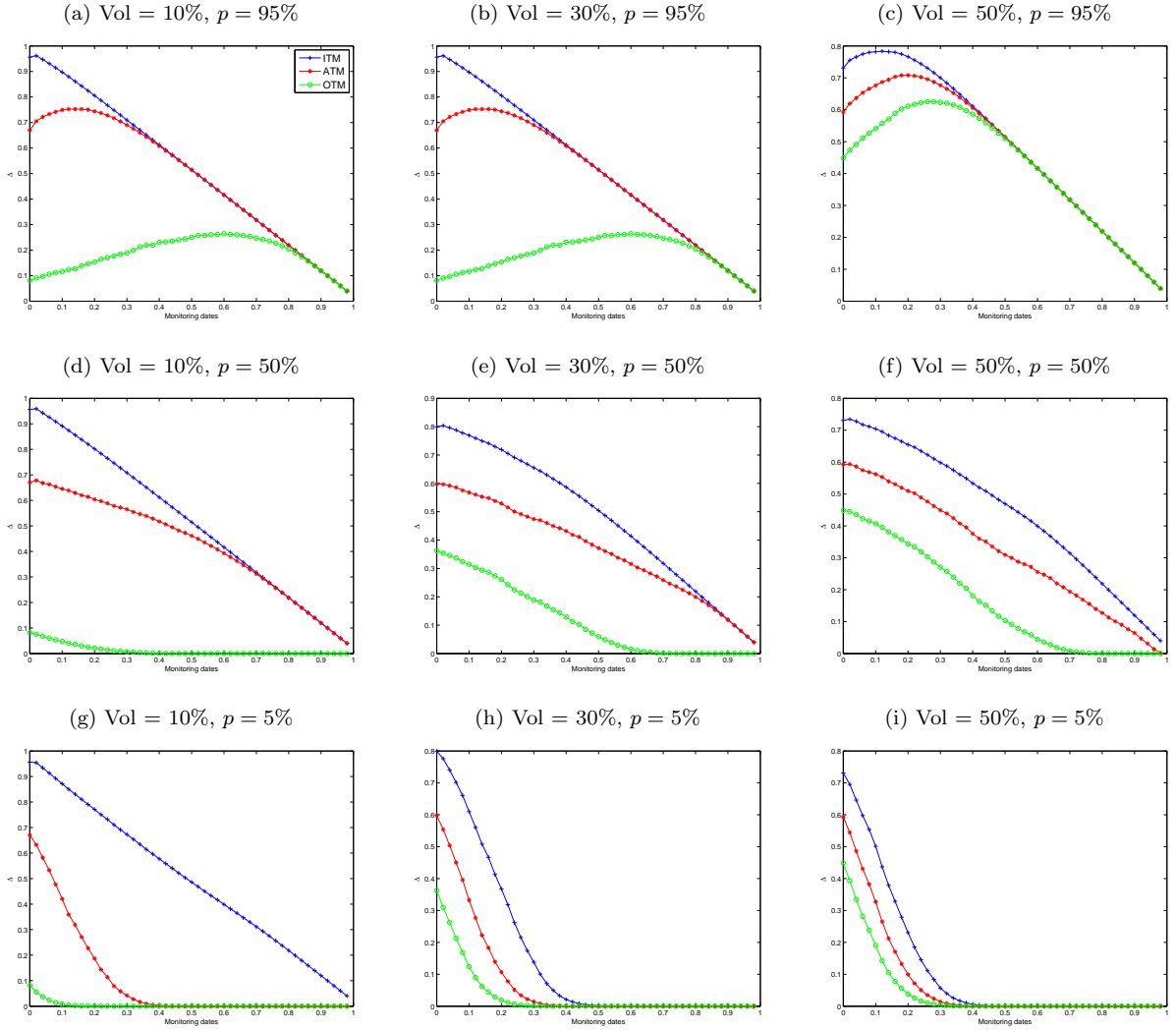
Figure 3
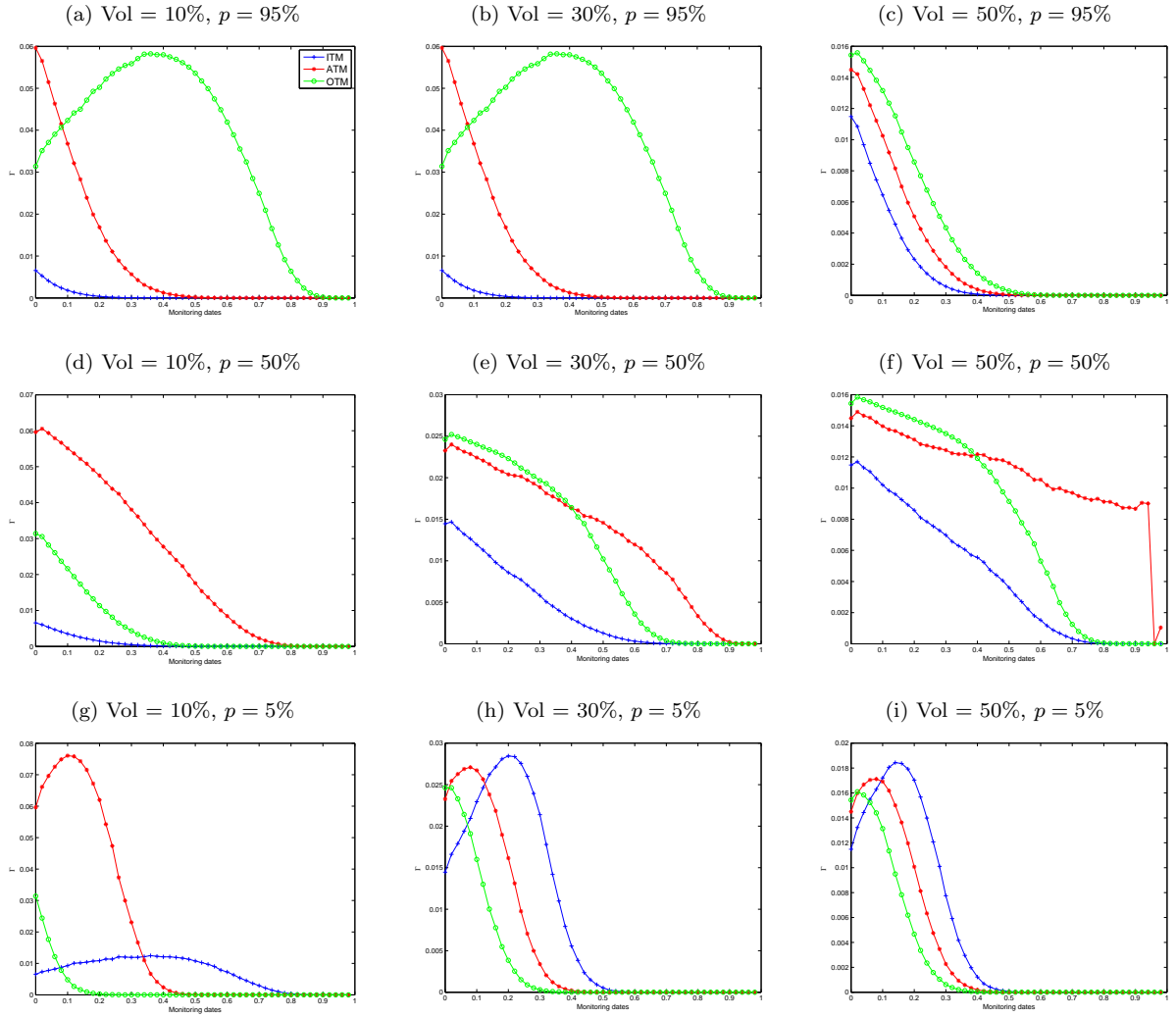Convergence patterns of computed vegas and vannas by backward recursion. NIG model.

Price sensitivity wrt NIG parameter ν

Price sensitivity wrt NIG parameter γ

Delta sensitivity wrt NIG parameter ν

Delta sensitivity wrt NIG parameter γ

[a] Convergence patterns of computed by backward recursion vegas and vannas with respect to the volatility parameters ν and γ of the NIG model for an at-the-money Asian call option ($S_0 = K = 100$) and the case of one-year log-return volatility Vol $= 0.1$ (see Panel (a) of Table 1). $\text{Vega}_N^{\text{NIG}}$, $\text{Vanna}_N^{\text{NIG}}$ denote the relevant sensitivities calculated by numerical implementation of the backward recursive integrals by discrete Fourier transform (see Černý and Kyriakou, 2011, Section 4) for N discretization points. $|\text{Vega}_N^{\text{NIG}} - \text{Vega}_{N/2}^{\text{NIG}}|$, $|\text{Vanna}_N^{\text{NIG}} - \text{Vanna}_{N/2}^{\text{NIG}}|$ are the absolute differences calculated for $N = 2^{15}, \ldots, 2^{19}$. Other parameters: $r = 0.04$, $T = 1$, $n = 50$.

Figure 4
Delta of Asian call option. NIG model.

(a) Vol = 10%, $p = 95\%$ (b) Vol = 30%, $p = 95\%$ (c) Vol = 50%, $p = 95\%$

(d) Vol = 10%, $p = 50\%$ (e) Vol = 30%, $p = 50\%$ (f) Vol = 50%, $p = 50\%$

(g) Vol = 10%, $p = 5\%$ (h) Vol = 30%, $p = 5\%$ (i) Vol = 50%, $p = 5\%$

[a] Delta of the arithmetic Asian call option over the lifetime of the contract. Quantiles trajectories obtained from 1,000 batches of 10,000 NIG paths observed at the reset dates of the Asian call option. One-year log-return volatilities Vol = $\{0.1, 0.3, 0.5\}$, strike prices $K = 90$ (in-the-money (ITM)), $K = 100$ (at-the-money (ATM)), $K = 110$ (out-of-the-money (OTM)), quantiles $p = \{0.05, 0.5, 0.95\}$. Model parameters: see Panel (a) of Table 1. Other parameters: $S_0 = 100$, $r = 0.04$, $T = 1$, $n = 50$.
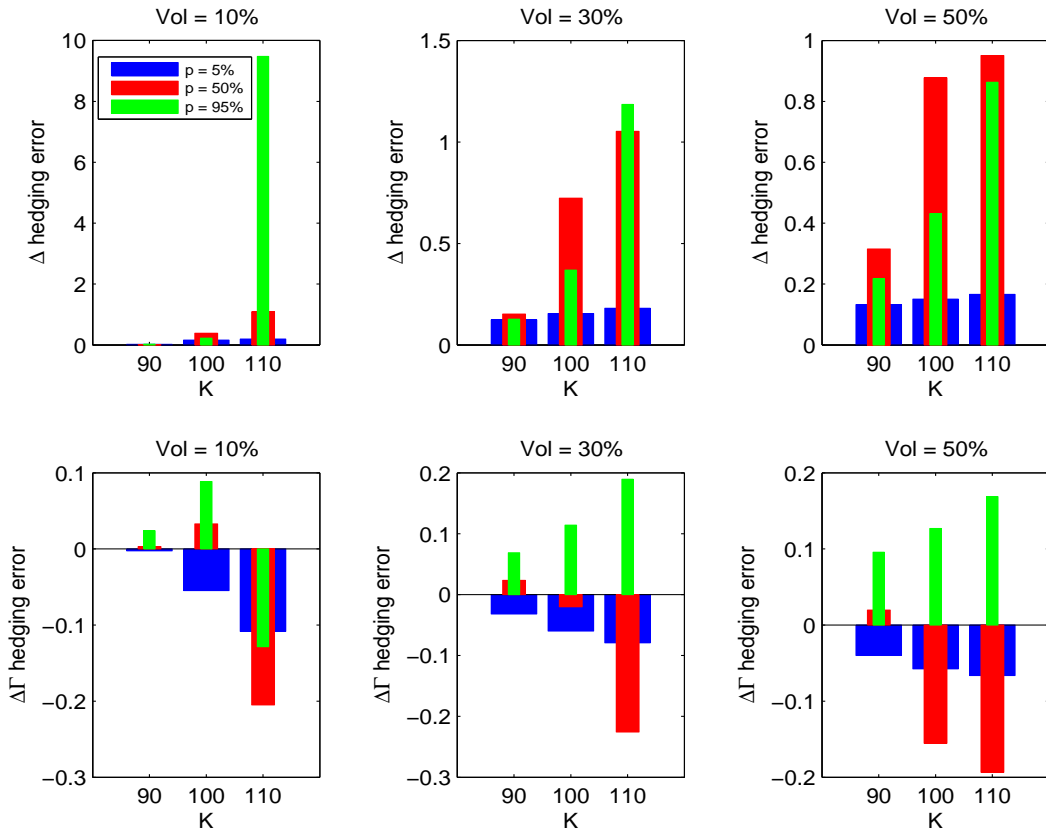
Figure 5
Gamma of Asian call option. NIG model.

(a) Vol = 10%, $p = 95\%$
(b) Vol = 30%, $p = 95\%$
(c) Vol = 50%, $p = 95\%$
(d) Vol = 10%, $p = 50\%$
(e) Vol = 30%, $p = 50\%$
(f) Vol = 50%, $p = 50\%$
(g) Vol = 10%, $p = 5\%$
(h) Vol = 30%, $p = 5\%$
(i) Vol = 50%, $p = 5\%$

[a] Gamma of the arithmetic Asian call option over the lifetime of the contract. Quantiles trajectories obtained from 1,000 batches of 10,000 NIG paths observed at the reset dates of the Asian call option. One-year log-return volatilities Vol = $\{0.1, 0.3, 0.5\}$, strike prices $K = 90$ (in-the-money (ITM)), $K = 100$ (at-the-money (ATM)), $K = 110$ (out-of-the-money (OTM)), quantiles $p = \{0.05, 0.5, 0.95\}$. Model parameters: see Panel (a) of Table 1. Other parameters: $S_0 = 100$, $r = 0.04$, $T = 1$, $n = 50$.
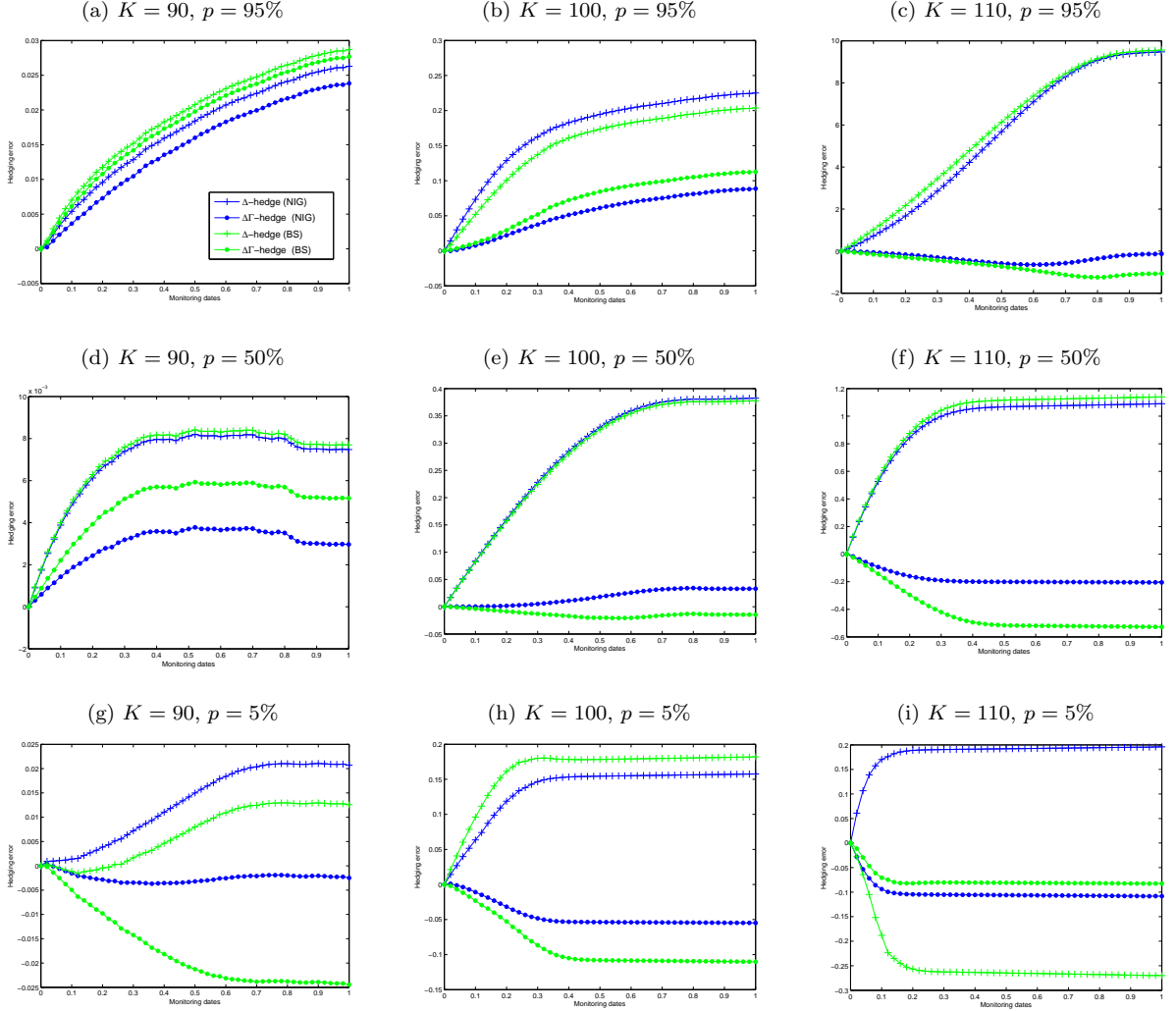
Figure 6
Hedging errors of delta hedge and delta-gamma hedge. NIG model.

[a] Δ hedging error: difference between the delta hedging portfolio and the option's terminal payoff, divided by the forward option premium. $\Delta\Gamma$ hedging error: difference between the delta-gamma hedging portfolio and the option's terminal payoff, divided by the forward option premium. Delta-gamma portfolio composition: European vanilla call option on S with maturity in 14 months and strike fixed at 95 (for the case of the Asian call struck at 90), 105 (for the case of the Asian call struck at 100) and 120 (for the case of the Asian call struck at 110), underlying asset (and risk free bond). Quantiles trajectories obtained from 1,000 batches of 10,000 NIG paths observed at the reset dates of the Asian call option. One-year log-return volatilities Vol $= \{0.1, 0.3, 0.5\}$, strike prices $K = \{90, 100, 110\}$, quantiles $p = \{0.05, 0.5, 0.95\}$. Model parameters: see Panel (a) of Table 1. Other parameters: $S_0 = 100$, $r = 0.04$, $T = 1$, $n = 50$.
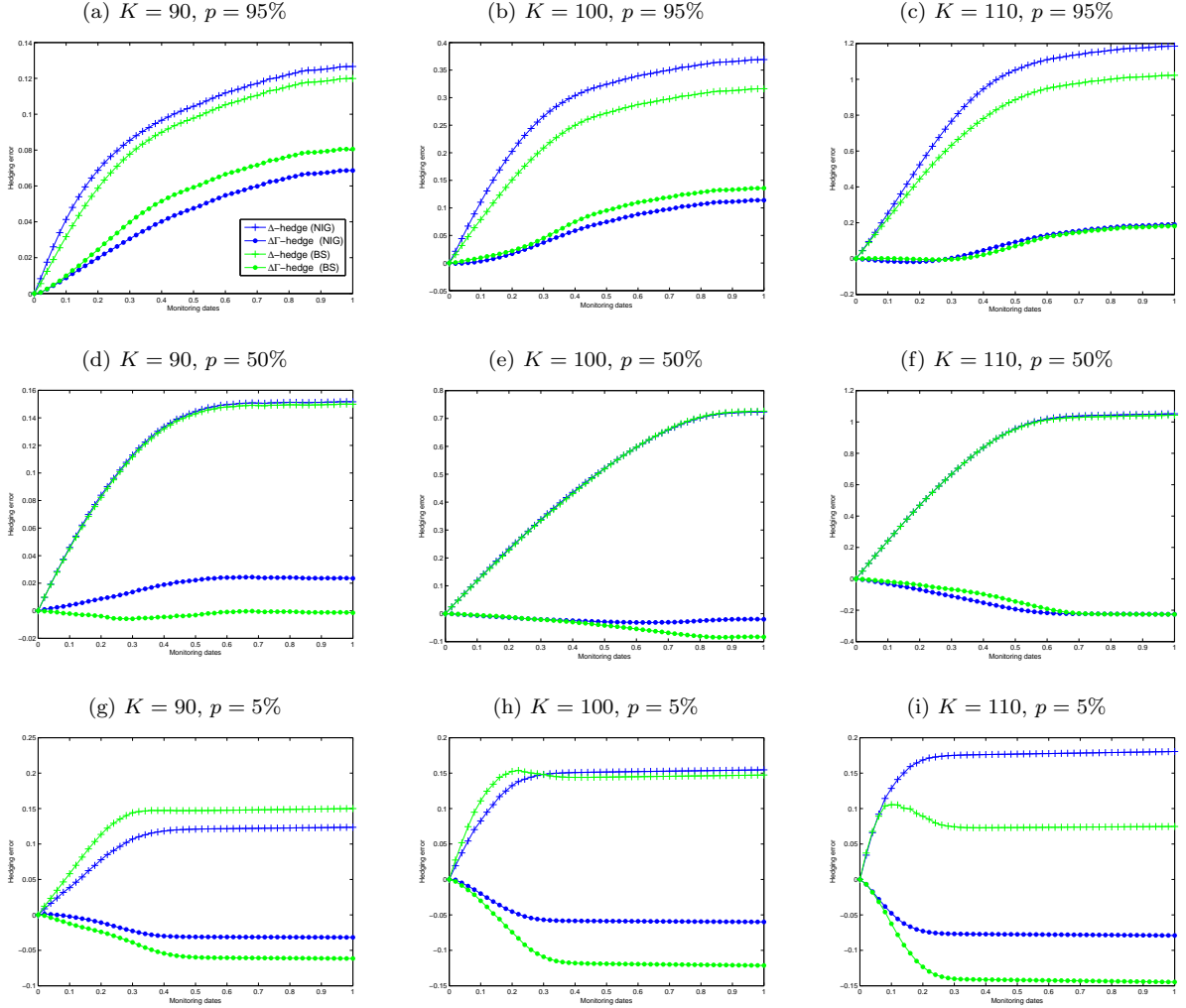
Figure 7
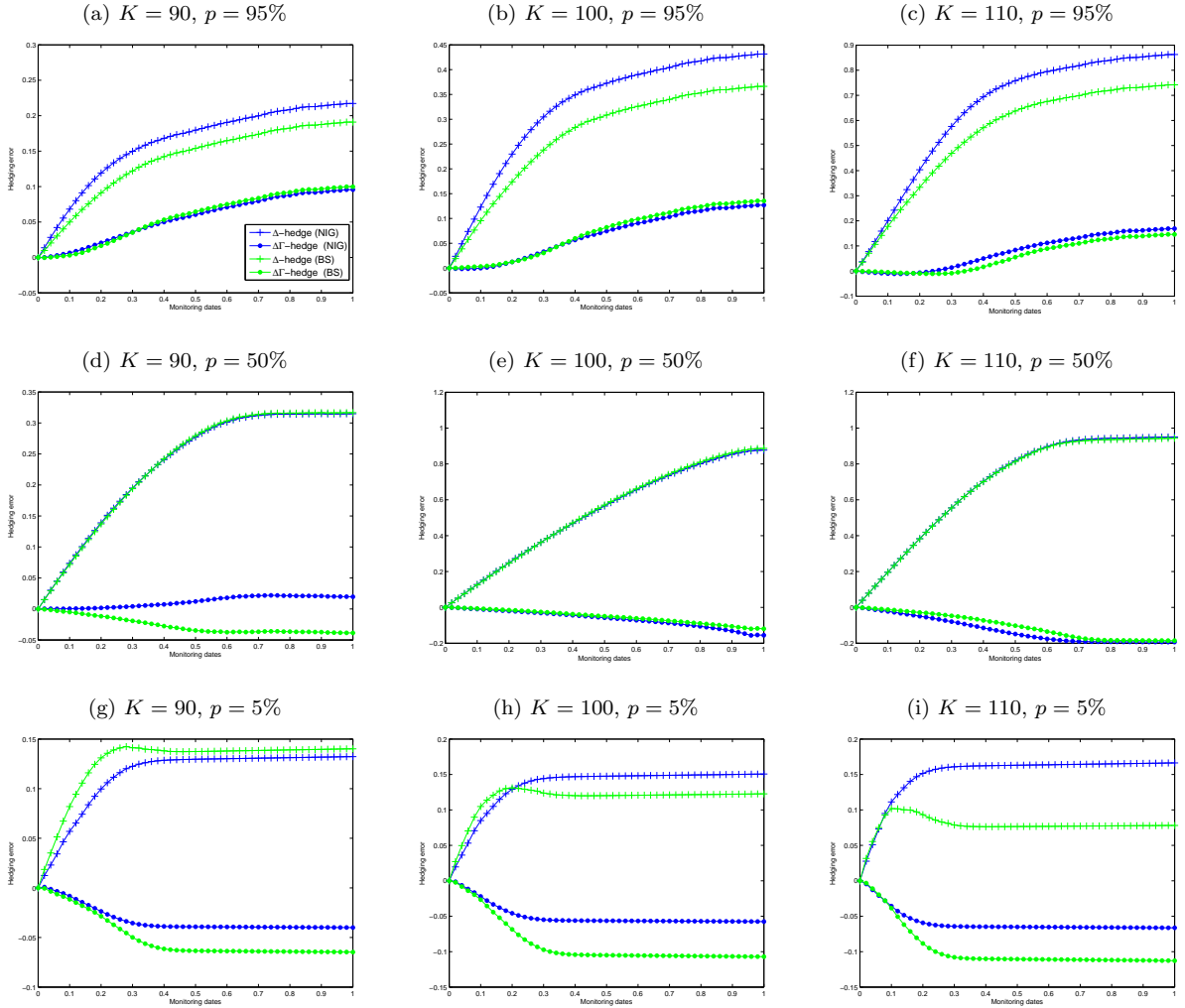Model error: NIG vs. Black–Scholes model. Vol = 10%.

[a] Hedging error: difference between the hedging portfolio at k^{th} monitoring date and the option price at the same date, divided by the forward option premium, $k = 1, \ldots, n$. $\Delta/\Delta\Gamma$-hedge (NIG): model delta (delta-gamma) hedging portfolio. $\Delta/\Delta\Gamma$-hedge (BS): Black–Scholes delta (delta-gamma) hedging portfolio. Delta-gamma portfolio composition: European vanilla call option on S with maturity in 14 months and strike fixed at 95 (for the case of the Asian call struck at 90), 105 (for the case of the Asian call struck at 100) and 120 (for the case of the Asian call struck at 110), underlying asset (and risk free bond). Quantiles trajectories obtained from 1,000 batches of 10,000 NIG paths observed at the reset dates of the Asian call option, quantiles $p = \{0.05, 0.5, 0.95\}$. Model parameters: see Panel (a) of Table 1. Other parameters: $S_0 = 100$, $r = 0.04$, $T = 1$, $n = 50$.

Figure 8
Model error: NIG vs. Black–Scholes model. Vol = 30%.

^{a} Hedging error: difference between the hedging portfolio at k^{th} monitoring date and the option price at the same date, divided by the forward option premium, $k = 1, \ldots, n$. $\Delta/\Delta\Gamma$-hedge (NIG): model delta (delta-gamma) hedging portfolio. $\Delta/\Delta\Gamma$-hedge (BS): Black–Scholes delta (delta-gamma) hedging portfolio. Delta-gamma portfolio composition: European vanilla call option on S with maturity in 14 months and strike fixed at 95 (for the case of the Asian call struck at 90), 105 (for the case of the Asian call struck at 100) and 120 (for the case of the Asian call struck at 110), underlying asset (and risk free bond). Quantiles trajectories obtained from 1,000 batches of 10,000 NIG paths observed at the reset dates of the Asian call option; quantiles $p = \{0.05, 0.5, 0.95\}$. Model parameters: see Panel (a) of Table 1. Other parameters: $S_0 = 100$, $r = 0.04$, $T = 1$, $n = 50$.

Figure 9

Model error: NIG vs. Black–Scholes model. Vol = 50%.

(a) $K = 90$, $p = 95\%$

(b) $K = 100$, $p = 95\%$

(c) $K = 110$, $p = 95\%$

(d) $K = 90$, $p = 50\%$

(e) $K = 100$, $p = 50\%$

(f) $K = 110$, $p = 50\%$

(g) $K = 90$, $p = 5\%$

(h) $K = 100$, $p = 5\%$

(i) $K = 110$, $p = 5\%$

[a] Hedging error: difference between the hedging portfolio at k^{th} monitoring date and the option price at the same date, divided by the forward option premium, $k = 1, \ldots, n$. $\Delta/\Delta\Gamma$-hedge (NIG): model delta (delta-gamma) hedging portfolio. $\Delta/\Delta\Gamma$-hedge (BS): Black–Scholes delta (delta-gamma) hedging portfolio. Delta-gamma portfolio composition: European vanilla call option on S with maturity in 14 months and strike fixed at 95 (for the case of the Asian call struck at 90), 105 (for the case of the Asian call struck at 100) and 120 (for the case of the Asian call struck at 110), underlying asset (and risk free bond). Quantiles trajectories obtained from 1,000 batches of 10,000 NIG paths observed at the reset dates of the Asian call option; quantiles $p = \{0.05, 0.5, 0.95\}$. Model parameters: see Panel (a) of Table 1. Other parameters: $S_0 = 100$, $r = 0.04$, $T = 1$, $n = 50$.